Molecular and Cellular Endocrinology 613 (2026) 112720

Contents lists available at ScienceDirect

Molecular and Cellular Endocrinology

journal homepage: www.elsevier.com/locate/mce

Estrogen therapies enhance mammary carcinogenesis in aging gerbil females under endocrine disruption

Thalles Fernando Rocha Ruiz [a,*], Stella Bicalho Silva [b], Vitor Grigio [b], Paula Rahal [b], Marília de Freitas Calmon [b], Patrícia Simone Leite Vilamaior [b], Ellen Cristina Rivas Leonel [c,d], Sebastião Roberto Taboga [a,b,**]

[a] Department of Structural and Functional Biology, Institute of Biology, University of Campinas (UNICAMP), Campinas, Brazil
[b] Department of Biology, Institute of Biosciences, Humanities and Exact Sciences, São Paulo State University, São José Do Rio Preto, SP, Brazil
[c] Department of Histology, Embryology and Cell Biology, Institute of Biological Sciences, Federal University of Goiás, Goiânia, Goiás, Brazil
[d] Animal Molecular and Cellular Biology Unit (AMCB), Louvain Institute of Biomolecular Science and Technology (LIBST), Ecole de Médecine Vétérinaire, Faculté de Sciences, UCLouvain, Belgium

ARTICLE INFO

Keywords:
Neoplasia
Menopause
BPA
Hormonal therapy
BRCA1
Cadherin

ABSTRACT

Breast cancer is closely associated with the hormonal sensitization that the mammary gland (MG) undergoes. We evaluated the effects of endogenous (E2) and synthetic (EE2) estrogens, commonly used as hormonal therapies during menopause, in a context of a pro-carcinogenic environment of endocrine disruption. This scenario was modeled to mimic the menopausal involution of the MG during aging in the Mongolian gerbil experimental model under previous bisphenol A exposure, during pregnancy and lactation. Our findings revealed significant remodeling of the epithelial compartment, characterized by increased branching density and loss of normal features, including decreased CD117+ luminal cells and loss of E-cadherin expression. Hormonal therapy with E2 or EE2 led to the development of epithelial lesions, characterized by an increase in invasive microcarcinomas and a decrease in basal (p63+α-SMA-) and myoepithelial (p63+α-SMA+) progenitor cells, contributing to increased neoplastic invasiveness. These changes were orchestrated by overexpression of EZH2 and a decrease in BRCA1, indicating a poor prognosis, especially for EE2. Furthermore, an imbalance between proliferation (PH-H3^{+} cells) and apoptosis (cleaved caspase 3) was observed in the MG of females treated with E2 and EE2. Additionally, distinct hormone receptor profiles were identified, with consistent upregulation of ERα and concomitant downregulation of ERβ and PR, particularly in EE2-treated MG. These alterations may contribute to the observed dysregulation of proliferation and apoptosis. Our results demonstrate that estrogenic hormonal therapies promote neoplastic progression of the aging MG previously subjected to endocrine disruption.

1. Introduction

Breast cancer classification relies on molecular markers and the progression pattern of epithelial lesions (Makki, 2015). The mammary gland (MG) is highly dynamic, undergoing significant structural changes throughout the reproductive cycle (Monteiro et al., 2020; Paine and Lewis, 2017; McCave et al., 2010). These changes are primarily orchestrated by ovarian hormones, estrogens and progesterone, which drive morphogenesis and are critical to both normal development (Mallepell et al., 2006; Dawson and Visvader, 2021) and could be crucial for carcinogenesis (Liao et al., 1998; Cheung et al., 2003). Estrogens stimulate epithelial proliferation and expansion of the MG epithelial surface (Dawson and Visvader, 2021) (Sternlicht et al., 2006; Gagniac et al., 2020). These periods of hormonal oscillations are known as windows of susceptibilities (Terry et al., 2019; Rodgers et al., 2018), since the remodeling resulting from these hormonal oscillations agrees with pro-neoplastic features (Del Pup et al., 2019). Compensation that prevents tumor progression occurs through elevated apoptotic pathways

* Corresponding author. Department of Biological Sciences, IBILCE, São Paulo State University (Unesp), Cristóvão Colombo St., 2255, Jardim Nazareth, São José do Rio Preto, São Paulo, 15054-000, Brazil.
** Corresponding author. Department of Biological Sciences, IBILCE, São Paulo State University (Unesp), Cristóvão Colombo St., 2255,Jardim Nazareth, São José do Rio Preto, São Paulo, 15054-000, Brazil.
E-mail addresses: tfrruiz@gmail.com (T.F.R. Ruiz), sebastiao.taboga@unesp.br (S.R. Taboga).

https://doi.org/10.1016/j.mce.2025.112720
Received 11 August 2025; Received in revised form 25 November 2025; Accepted 12 December 2025
Available online 17 December 2025

by the enhancement of tumor suppressor genes, such as *BRCA1*, *p53*, and histone methylation proteins (V Fernandez et al., 2012; Freneaux et al., 2000) that control the exacerbated remodeling of the epithelial and stromal compartments (Dawson and Visvader, 2021; Inman et al., 2015). This preventive machinery may have deficiencies due to several processes and agents to which women are ubiquitously exposed and susceptible.

Aging remodels MG as well, as during menopause, a drastic decrease in hormonal levels induces the involution of the MG epithelium (Butler and Santoro, 2011; Lobo, 2017). However, in addition to these intra-mammary events, women at this stage of life suffer from side effects of hormonal decline, which are commonly resolved with exogenous hormone supplementation (Raafat et al., 1999; Santen et al., 2010; Sood et al., 2014). Estrogenic compounds are the basis for these medications or hormonal therapies, as they greatly influence reproductive organs and behavioral cycles (Stuenkel, 2015). Despite their supplementary indication, these compounds, similarly to endogenous and synthetic estrogens, may offer a risk for developing neoplastic features in the MG (Lobo, 2017; Marchese and Silva, 2012; Gomez et al., 2017). By activating proliferative pathways and disrupting their compensatory balance through anti-proliferative pathways, the development of ductal lesions and carcinomas is commonly reported in women at these stages (Hunter, 2017). These changes are mainly linked to alterations in the epithelial compartment's profile, as its cell types are estrogen-sensitive (Terry et al., 2019). Myoepithelial and basal cells support the development and homeostasis of luminal cells derived from progenitor lineages, which are essential for the self-renewal of MG (Stingl et al., 2005; Pellacani et al., 2016; Shalabi et al., 2021). Changes in this profile signal disordered development and, consequently, neoplasia in this gland (Ingthorsson et al., 2015), which can be enhanced in different scenarios, such as exposure to deregulatory agents.

Endocrine disruptors have recently been defined as a potential trigger of breast cancer. Studies introduced in past decades indicate that exogenous chemical compounds affect endocrine pathways, which interfere with gland development (Khan et al., 2021; Segovia-Mendoza et al., 2020; Bleak and Calaf, 2021). The endocrine-disrupting chemicals (EDC) are found in several environments, and constant exposure to them causes irreversible pathological conditions (Paterni et al., 2017; Vabre et al., 2017). Bisphenol A (BPA) is a plastic-derived EDC that has been extensively explored due to its wide distribution and origins (Corrales et al., 2015). The effects reported for BPA are related to xenoestrogen activity, impairing the main development of the MG (Dumitrascu et al., 2020; Soto et al., 2013), and binds ubiquitously to several receptors (Shafei et al., 2018). BPA leads to tissue remodeling that triggers endocrine-related MG cancer, altering cellular characteristics and promoting a pro-tumor microenvironment (Dumitrascu et al., 2020; Buteau-Lozano et al., 2008; Bhan et al., 2014). Among the main impacts of BPA, changes at the epigenetic level stand out, as these can alter cascades and molecular pathways that directly influence tumor development (Fernandez and Russo, 2010; Doshi et al., 2011). These changes can be verified through the expression of epigenetic modulators that are related to gene overexpression and silencing, such as EZH2 (Bhan et al., 2014; Leonel et al., 2020a), and confirmed by altered BRCA1 expression (Qin et al., 2012; Atlas and Dimitrova, 2019), relevant for the prognosis of breast cancer.

Estrogenic therapies could be potential carcinogenic factors under endocrine disruption. We hypothesized that BPA exposure of mothers during pregnancy and lactation induces the onset of mammary carcinogenesis at aging and hormonal therapies (Ruiz et al., 2021a, 2021b). In addition to tumoral invasive features, the MG presents a high responsivity to estrogens due to hormonal receptor expression (Kanaya et al., 2019a). Thus, our objective was to assess the carcinogenic potential of two standard estrogen compounds: endogenous 17β-estradiol (E2) and synthetic 17α-ethynylestradiol (EE2) (Kuhl, 2005; Stuenkel, 2015) in the MG of Mongolian gerbil (experimental model) mothers previously exposed to BPA-induced endocrine disruption, with treatments and analyses conducted during aging. The Mongolian gerbil (*Meriones unguiculatus*) provides a valuable model for hormone-related MG research. Previous work demonstrated that BPA exposure during sensitive windows, such as pregnancy and lactation, induces persistent epithelial remodeling and later carcinogenic features in aged females (Ruiz et al., 2021a, 2022; Leonel et al., 2020b, 2020c), supporting its use for studying long-term endocrine effects. The gerbil thus offers a complementary system to mouse and rat models for investigating estrogenic and endocrine disruption pathways (Ruiz et al., 2023a). Our study revealed significant changes in epithelial compartments and cell rearrangement, as well as imbalances in proliferative indices and in the expression of EZH2 and BRCA1.

2. Materials and methods

2.1. Animals and experimental design

Fifty female Mongolian gerbils were housed with fertile males (3 months old) under a light/dark cycle (12h/12h) in a temperature-controlled room (24 °C) and *ad libitum* feeding. After pregnancy was confirmed through the presence of sperm cells in the vaginal smear, each female was exposed to daily pro-carcinogenic oral doses of BPA (50 μg/kg/day) diluted in 0.1 ml corn oil from the 8th day of pregnancy to the 21st day of lactation, for a total of 39 days of exposure. This treatment in both windows of susceptibility (pregnancy and lactation) aimed to induce the onset of carcinogenesis during aging (Ruiz et al., 2021c). Then, at 12 months age, BPA-exposed females were subdivided into four experimental groups (n = 15/group): *EDC* – females exposed only to BPA during pregnancy/lactation, with no post-treatment; *E2* – BPA-exposed females were treated daily by gavage with 17β-estradiol (0.5 mg/kg) (Sigma-Aldrich, E8875) diluted in 0.1 ml corn oil (Stuenkel et al., 2015; Hodis et al., 2016), for 6 months; and *EE2* – BPA-exposed females were treated by gavage with 17α-ethynilestradiol (35 μg/kg) (Sigma-Aldrich, E4876) diluted in 0.1 ml corn oil (Ruggiero and Likis, 2002; De Leo et al., 2016) for 6 months. A control group was also established with uniparous females, one pregnancy only (n = 15), not treated. Chosen doses remain hormonal therapy dosages for estrogen replacement (Stuenkel, 2015) or perimenopause symptoms (Ruggiero and Likis, 2002; De Leo et al., 2016), described for E2 and EE2, respectively. For estrogenic compounds and their doses, the pharmacokinetic aspects of oral absorption were considered (Hodis et al., 2016).

All females were euthanized at 18 months of age (aging period), and inguinal MGs were collected and destined to fixation either in 4 % paraformaldehyde (histopathology) or Kahle's (Whole mounted) fixative solutions or frozen at −80 °C (Western Blotting).

2.2. Histopathological analysis

2.2.1. Mammary gland whole mounts

MG whole mounts (WM) were prepared during euthanasia. Methods and preparations were based on Stanko and Fenton (2017) and Tolg et al. (2018). Collected inguinal MG (n = 5/group) were placed in Fisherbrand™ Superfrost™ Plus Microscope Slides and fixed in Kahle's fixative (37 % formaldehyde, 95 % ethanol, Acetic acid) for 4 h. WM slides were stained overnight in 2 % Carmine-Potassium Alum, and then dehydrated with ethanol and cleared with xylene. Slides were sealed and observed under an Olympus® BX60 microscope.

For quantification of morphometric parameters in WM slides, 15 random fields (200x magnification) per animal were measured with a grid (200 crosshairs) in each image. Volume fraction of ductal structures, alveolar buds (terminal regions of ductal structures, not expanded), and terminal end buds (TEB-like structures) (bulb-shaped structures) was obtained. The percentage of the total volume fraction per structure was evaluated as (number of crosshairs/total crosshairs) × 100.

2.2.2. Sholl's analysis

Branching density of MG was analyzed by Sholl's method, as described in Stanko et al. (2015) and Stanko and Fenton (2017). This parameter indicates the level and complexity of MG development. WM slides were scanned in an Olympus BX61VS system, and images were captured at the same magnification. Using the ImageJ software, glandular portions of MG were selected, excluding the lymph node. Skeletonized images were obtained after color channel separation and overlaid onto the original image to compare the structures selected by the software. The ImageJ plugin "Advanced Sholl Analysis" was used to run the analysis and obtain the following parameters: enclosing radius (longitudinal growth of MG epithelium); mammary epithelial area (*MEA* – considering all mammary perimeter selected); *N* (number of radial intersections, referring to ductal tree); and Sholl coefficient regression (*k* – branching complexity of glandular epithelium). All data were plotted in Table 1.

2.2.3. Histological analyses

Epithelial lesions and alterations were evaluated under histological slides. Samples were embedded in paraffin and sectioned (4 μm). For histopathological analysis (Hematoxylin-Eosin staining and immunohistochemistry), sections were obtained at three different depths and analyzed. Slides were stained with Hematoxylin-Eosin; an immunohistochemistry assay was performed to detect the proteins. General immunohistochemistry and double-immunohistochemistry procedures were performed according to the following protocols: samples were deparaffinized and rehydrated, then antigen-retrieved with 10 mM Citrate Buffer (pH 5.8) at 95–99 °C. After, the slides were destined to endogenous peroxidase blockage with 10 % H_2O_2 in methanol. Endogenous protein blockage was performed with 5 % skimmed milk or 10 % BSA in wash buffer. Primary antibody incubation was overnight; for double-immunohistochemistry, two antibodies of different hosts were incubated together. Dilution and identification of antibodies were as follows: BRCA1 (MA1-23164, Invitrogen, 1:75, mouse monoclonal); Caspase 3 (E−8, Santa Cruz Biotechnology, 1:50, mouse monoclonal); CD117/c-Kit (34–8800, Invitrogen, 1:100, rabbit monoclonal); Cleaved Caspase 3 (D175, Elabscience, 1:75, rabbit polyclonal); EZH2 (D2C9, Cell Signaling, 1:75, rabbit monoclonal); p63 (D-9, Santa Cruz Biotechnology, 1:75, mouse monoclonal); Pan-cadherin (4086, Cell Signaling, 1:100, rabbit monoclonal); phosphor-histone H3 (PHH3 9701, Cell Signaling, 1:75, rabbit monoclonal); smooth muscle α-Actin (sc-130617, Santa Cruz Biotechnology, 1:100, mouse monoclonal; or 17H19L35, Invitrogen, 1:100, rabbit monoclonal); Vimentin (D21H3, Cell Signaling, 1:100, rabbit monoclonal). For immunohistochemistry, detection of primary antibodies was performed by Novolink™ Polymer detection system (Leica Biosystems), and positive reaction was observed by 3–30 diaminobenzidine tetrahydrochloride (DAB) (Novolink™ DAB, RE7270-CE, Leica Biosystems Ltd.). For double immunohistochemistry, antibodies from different hosts were detected using Multiplex DetectionTM MACH 2 Double Stain 1 (Biocare Medical, Concord, CA) and reacted with DAB and Alkaline Phosphatase (AP) using the Vulcan Fast Red Chromogen Kit 2 (Biocare Medical). All slides were counterstained with hematoxylin and mounted. Whole sections were scanned in an Olympus BX60 Scanner Microscope and analyzed in OlyVIA software (v. 4.1). Analyses were performed in QuPath software, considering only epithelial cells, with calibration steps used to select and separate the epithelial and stromal compartments.

2.2.4. Analysis of histopathological alterations

Epithelium was evaluated in whole scanned sections (3 different depths), and identification followed the classifications (Duivenvoorden et al., 2018): normal epithelium, hyperplasic foci (>2 layers of luminal epithelial cells showing myoepithelial layer integrity), ductal carcinoma in situ (loss of lumen shape due to proliferation of epithelial cells, high epithelial content, and myoepithelial layer integrity – noninvasive), and microinvasive carcinoma (loss or rupture of myoepithelial layer with epithelial cell proliferation, including carcinomas poor, moderate and high differentiated). These features were evaluated in two slides per animal, stained with H&E and with double-immunohistochemistry for α-SMA (smooth muscle actin, for myoepithelial cells) and CD117 (for luminal cells). The incidence of epithelial lesions was quantified as the number of alterations per total epithelial focus observed per section, expressed as the percentage of each alteration.

For Pan-cadherin immunostaining, the deconvolution method was applied to the samples using ImageJ. Five fields (10 ×) per animal (n = 4) were analyzed per section. Image deconvolution was performed with the Color Deconvolution plugin to separate the DAB and hematoxylin channels. The DAB channel was used to quantify Pan-cadherin immunoreactivity, and the relative positive area was measured using a fixed threshold to ensure consistent analysis across samples.

To identify basal/luminal progenitors (p63+αSMA-) and myoepithelial progenitor cells (αSMA+), a double immunofluorescence assay was also employed. Slides were deparaffinized and rehydrated; subsequently, antigen retrieval was performed with 100 mM Citrate buffer (98 °C), followed by PBS washes. Non-specific proteins were blocked with 5 % skimmed milk for 1 h, followed by overnight incubation with primary antibodies (1:50), with the same antibodies employed in immunohistochemistry. Secondary antibodies incubation was performed for 2 h, using FITC anti-mouse (sc-2010, 1:100, Santa Cruz Biotechnology, USA) and Texas Red anti-rabbit (sc-2780, 1:100, Santa Cruz Biotechnology, USA). The slides were mounted with a DAPI mounting medium (Fluoroshield™ with DAPI, F6057, histology

Table 1
Whole-mounted morphometric analysis (mean ± SEM).

	Control	EDC	E2	EE2
Volume Fraction (%)				
Alveolar buds	26.72 ± 3.689^{ab}	29.45 ± 5.436^{a}	21.5 ± 4.265^{b}	15.72 ± 3.997^{c}
TEB-like structures	11.78 ± 3.384^{c}	22.5 ± 3.449^{b}	21.11 ± 5.856^{b}	31.28 ± 7.388^{a}
Ducts	28.78 ± 6.377^{a}	29.31 ± 6.808^{a}	12.83 ± 5.562^{b}	17.39 ± 3.833^{b}
Sholl Analysis				
Enclosing radius (mm)	5.875 ± 2.4^{c}	16.62 ± 2.665^{ab}	12.93 ± 2.364^{b}	14.89 ± 1.851^{b}
N	984.1 ± 84.21^{c}	2940 ± 473.3^{b}	2983 ± 558.5^{b}	4099 ± 456.9^{a}
MEA (mm^2)	74.35 ± 9.316^{b}	135.5 ± 25.71^{a}	168 ± 41.11^{a}	158.9 ± 28.28^{a}
Branching density (N/MEA)	13.43 ± 2.003^{c}	22.87 ± 8.06^{ab}	18.68 ± 5.31^{bc}	26.3 ± 4.331^{ab}
k	0.573 ± 0.081^{a}	0.453 ± 0.133^{b}	0.426 ± 0.152^{b}	0.260 ± 0.054^{b}

Enclosing radius (mm).
N: number of intersections.
MEA: mammary epithelial area.
k: Sholl regression coefficient.
a,b,c superscript letters indicate significative differences among groups by ANOVA analysis for parametric or non-parametric data.

mounting medium, Merck, Darmstadt, Germany), to detect the nuclei. Analyses were performed in 15 random images/fields per animal and presented as a percentage of epithelial cells expressing or not both markers.

2.2.5. H-score

To evaluate the intensity of EZH2 and BRCA1 staining as a significant result for histopathology (Biondi et al., 2021). The H-score of these proteins was quantified among groups. Three sections per animal were analyzed, and epithelium positivity was considered for H-score analysis by the QuPath® tissue separation method. The H-score consisted of the staining intensity (0–3; light to strong staining) of each cell, considering the percentage of positive cells (0–100 %). H-score was calculated by [1 x (% cells^{1+}) + 2 x (% cells^{2+}) + 3 x (% cells^{3+})], resulting in values between [0–300] scores.

2.3. Western Blotting analysis

Molecular analyses were performed with MG frozen at −80 °C. The protocol followed the previously described steps for MG in Mongolian gerbils (Leonel et al., 2020b; Ruiz et al., 2023b). From MG, protein extracts were obtained by tissue digestion using RIPA lysis buffer (Merck Millipore), adding a Protease/Phosphatase Inhibitor Cocktail (1:100). Total protein concentration was quantified using the BCA Protein Assay kit (Pierce BCA Protein Assay Kit, ThermoFischer Scientific, Rockford, IL, USA). After this step, protein samples (20 μg) were subjected to SDS-PAGE (90V) and transferred to nitrocellulose membranes (Amersham Protran, 10,600,003, GE Healthcare). Samples were loaded into the gel wells in a randomized order, rather than grouped by experimental condition, to minimize potential loading or detection bias. An immunoblotting assay was performed with transferred nitrocellulose membranes. Non-specific proteins were blocked with 5 % skimmed milk in TBS-0.1 % Tween followed by incubation with primary antibodies overnight (4 °C): BRCA1 (MA1-23164, Invitrogen, 1:1000, mouse monoclonal); Caspase 3 (E−8, Santa Cruz Biotechnology, 1:1000, mouse monoclonal); EZH2 (D2C9, Cell Signaling, 1:1000, rabbit monoclonal); Pan-cadherin (4086, Cell Signaling, 1:2000, rabbit monoclonal). After, membranes were incubated with corresponding secondary antibodies (Anti-mouse IgG, HRP-linked Antibody, #7076, 1:2000, Cell Signaling or Anti-rabbit IgG, HRP-linked Antibody, #7074, 1:2000, Cell Signaling) and detection was performed by chemiluminescent method (Pierce ECL detection substrate solution, ThermoFischer, Rockford, IL, USA). Photodocumented membranes were analyzed using ImageJ software (version 1.52a, Wayne Rasband, NIH, USA) to quantify protein band density. Normalization was performed with β-actin (4967, Cell Signaling, 1:1000, rabbit monoclonal), and results were expressed as the relative density of the target protein to the endogenous protein.

2.4. Statistical analysis

Data analyses were performed using GraphPad Prism 8.00 (Windows). For stereology, immunohistochemistry, and Western Blotting, normality was assessed using the Kolmogorov-Smirnov test. One-way ANOVA was employed, followed by Tukey's test for parametric data; and Kruskal-Wallis's test, followed by Dunn's test, was applied for non-parametric data. Significant comparative analysis ($p < 0.05$).

2.5. Ethical statements

All animal experiments followed ARRIVE guidelines (https://arriveguidelines.org/) under protocol of the Ethical Institutional Committee (Prot. Num. 235/2022).

3. Results

3.1. Estrogens promoted morphometric and histopathological alterations in MG during aging

To determine alterations in the alveolar buds, TEB-like structures, ducts, and branching pattern of MG with different estrogenic therapies, stereological analysis in whole-mounted slides was performed (Fig. 1A–D). Duct frequency was decreased in E2 and EE2 compared to the control and EDC groups (Fig. 1 B). Females exposed to *EE2* presented a high-density percentage of TEB-like structures compared to control, *E2,* and *EDC* (Fig. 1 B). Sholl analysis (Fig. 1C) aided in determining branching density among groups, presented by the Sholl coefficient (*k*). Enhanced branching was found in *EDC* and *EE2*-exposed females due to enhanced values of branching density (N/MEA) analysis compared to the control group (Fig. 1D–D') (details in Table 1).

To assess alterations in the epithelial compartment, histopathological analysis was performed to assess the integrity of MG epithelia (Fig. 1E–F). Normal epithelial features were frequently observed in *control* MG and reduced in response to estrogenic treatments. However, hyperplasia, DCIS, and microinvasive carcinoma lesions were enhanced under endocrine disruption and estrogenic therapies (Fig. 1E). Hyperplasia incidence was enhanced in all treated groups compared to the control. E2 showed an increase in hyperplastic frequency compared to all treatments; also, EDC and EE2 increased hyperplastic incidence compared to the control group (Fig. 1E). The DCIS percentage in MG was higher in EDC and EE2 than in *E2*-exposed females. DCIS was based on α-SMA positivity to detect myoepithelial cells (Fig. 1F). Microinvasive carcinoma did not present a myoepithelial cell layer and was absent in control MG (Fig. 1F). In *EE2-exposed* females, microinvasive carcinoma was increased, in which MG presented values over 9 % of total epithelial structures (Fig. 1E), compared to control and *EDC*.

Luminal epithelial cells expressing CD117 were decreased in all MG under endocrine disruption (Fig. 2A–B). *EE2* presented a drastic decrease in CD117^{+} cells compared to other groups. Evaluation of epithelial integrity was also performed by pan-cadherin expression in MG (Fig. 2B–C). As predicted by CD117 expression, endocrine disruption promoted a decrease in the expression of cadherin epithelial structures (Fig. 2B–C). Generally, neoplastic features presented negative or weak immunoreactivity for pan-cadherin. A significant reduction in the pan-cadherin-positive area was observed in the mammary glands of E2-and EE2-exposed animals compared with the control group (Fig. 2C). Quantitative analysis of the deconvoluted images showed that the Pan-cadherin-positive area was 35.2 % ± 4.8 in controls, 32.5 % ± 3.9 in the EDC group, 17.6 % ± 2.7 in the E2 group, and 14.3 % ± 2.1 in the EE2 group (mean ± SEM, n = 4). The pan-cadherin protein level decreased only in EE2 samples, with a drastic decrease compared to other groups (Fig. 2D). This was reflected in the Western Blotting assay, where the amount of pan-cadherin (~110 kDa) was diminished in *EE2* (Fig. 2D–E).

The expression of key proteins of progenitor differentiation also evaluated damage in the epithelial compartment. Nuclear p63 (p63n) (Fig. 2F–G) indicates basal progenitor clusters for epithelial cells (p63n^{+}αSMA^{-}) and myoepithelial progenitor cells (p63n^{+}αSMA^{+}) (Fig. 2H), evaluated by double immunofluorescence assay (Fig. 2I). Total p63n was decreased under EE2 treatment compared with all experimental groups (Fig. 2F). Basal/Luminal progenitor cells (p63n^{+}αSMA^{-}) cluster decreased in MG of *E2* and *EE2* (Fig. 2G) in comparison to *EDC*. For myoepithelial progenitor cells (p63n^{+}αSMA^{+}), *EE2* females showed a reduction in comparison to the control (Fig. 2 G).

3.2. Epithelial-mesenchymal transition (EMT) parameters were enhanced in the MG under E2 and EE2 therapies

Due to the increased incidence of carcinoma observed in the treated groups (as presented in the previous section), EMT was evaluated by EZH2 and BRCA1 expression (Fig. 3A) (Li et al., 2020a; Cho et al., 2019;

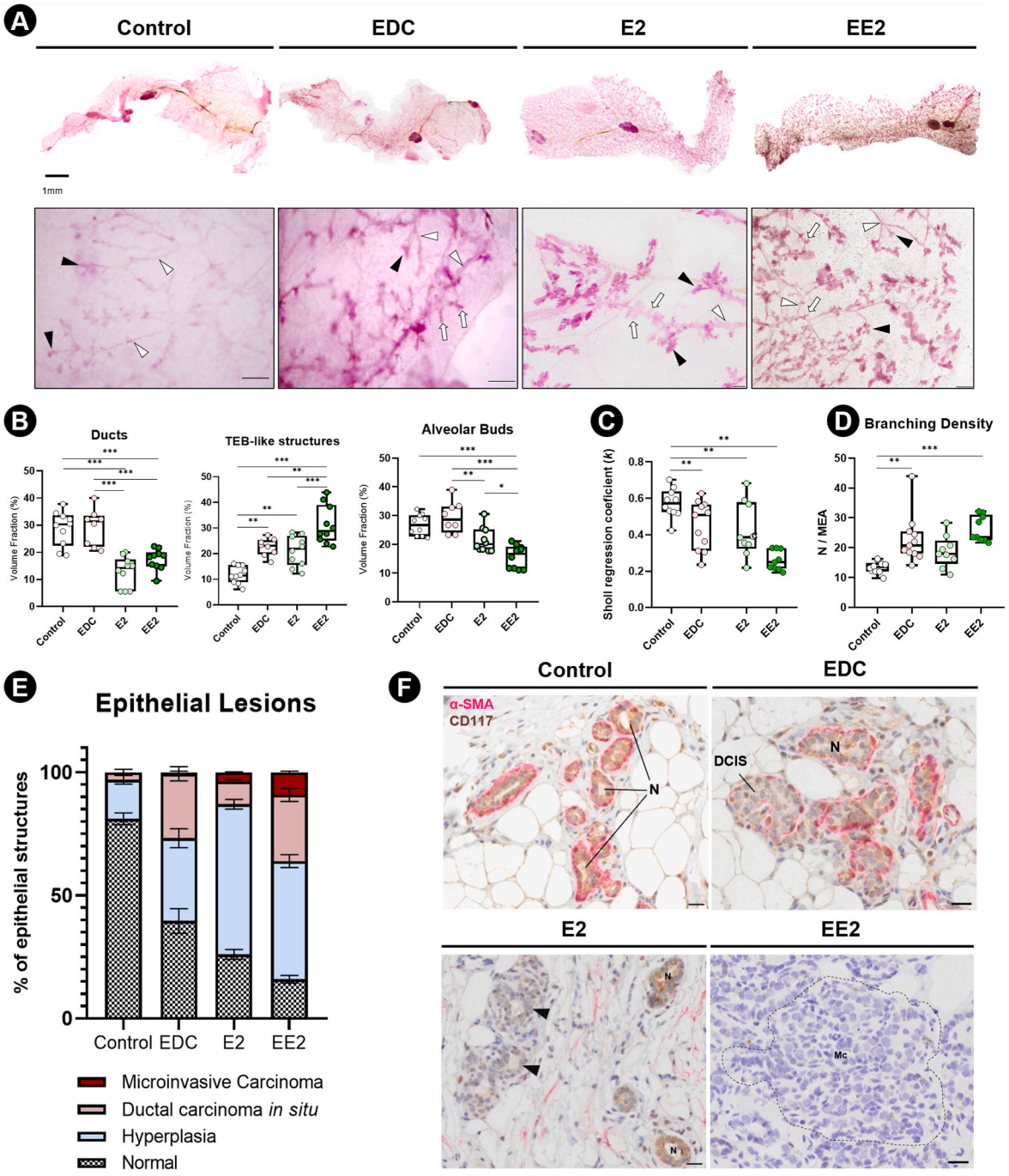

Fig. 1. General morphology of the MG. **(A)** Whole-mount images. **(B)** Volume fraction of ducts, terminal end bud (TEB)-like structures, and alveolar buds plotted as percentages. **(C)** Sholl regression coefficient (k), representing the decline in ductal insertions; lower values indicate increased branching complexity. **(D)** Branching density, quantifying the extent of epithelial network proliferation into the fat pad. **(E)** The distribution of epithelial lesions is shown as the percentage of total epithelial foci per slide, categorized by lesion type. **(F)** Representative double immunohistochemistry images display CD117 (a luminal marker, brown) and α-SMA (a myoepithelial marker, pink), illustrating epithelial features across different groups: normal alveoli (N); ductal carcinoma in situ (DCIS); arrowheads in the E2 group highlight the loss of CD117+ cells in alveoli-like structures alongside normal ones; in EE2 groups, microinvasive carcinoma (Mc - *dotted line*) did not express CD117 nor α-SMA. *Statistical representation* (*among groups*): $^{*}P < 0.05$, $^{**}P < 0.01$, and $^{***}P < 0.001$. *Scale Bars*: (A) 500 μm; (F) 20 μm.

Bai et al., 2022; Landragin et al., 2025), as well as by vimentin and pan-cytokeratin expression in MG epithelium (Fig. 3B). Both estrogenic therapies increased EZH2^{+} cells compared to the control and *EDC* groups (Fig. 3C). The EZH2 evaluation was also performed using an H-score (p ANOVA <0.005) based on staining intensity (Fig. 3 *inset*). Endocrine disruption enhanced the H-score, with estrogens showing increased values for this parameter: *E2* (129.5 ± 13.17) and *EE2* (136.8 ± 16.49), compared to the *control* group (5.17 ± 1.18) and the *EDC* group (97.44 ± 5.42). In contrast, BRCA1 nuclear expression in epithelial cells demonstrated a reduction in endocrine-disrupted MG (Fig. 3D). Females treated with *E2* and *EE2* presented a drastic reduction in BRCA1^{+} cells. This status was reflected in the H-score (p ANOVA <0.005) (Fig. 3D *inset*), in which BRCA1^{+} levels in MG under endocrine disruption was lower than the cutoff (score 100) - *EDC* (49.61 ± 5.36), *E2* (34.22 ± 3.94), and *EE2* (13.69 ± 4.69)-, contrarily from control MG (control: 141.5 ± 14.1). WB analysis confirmed that the amount of EZH2

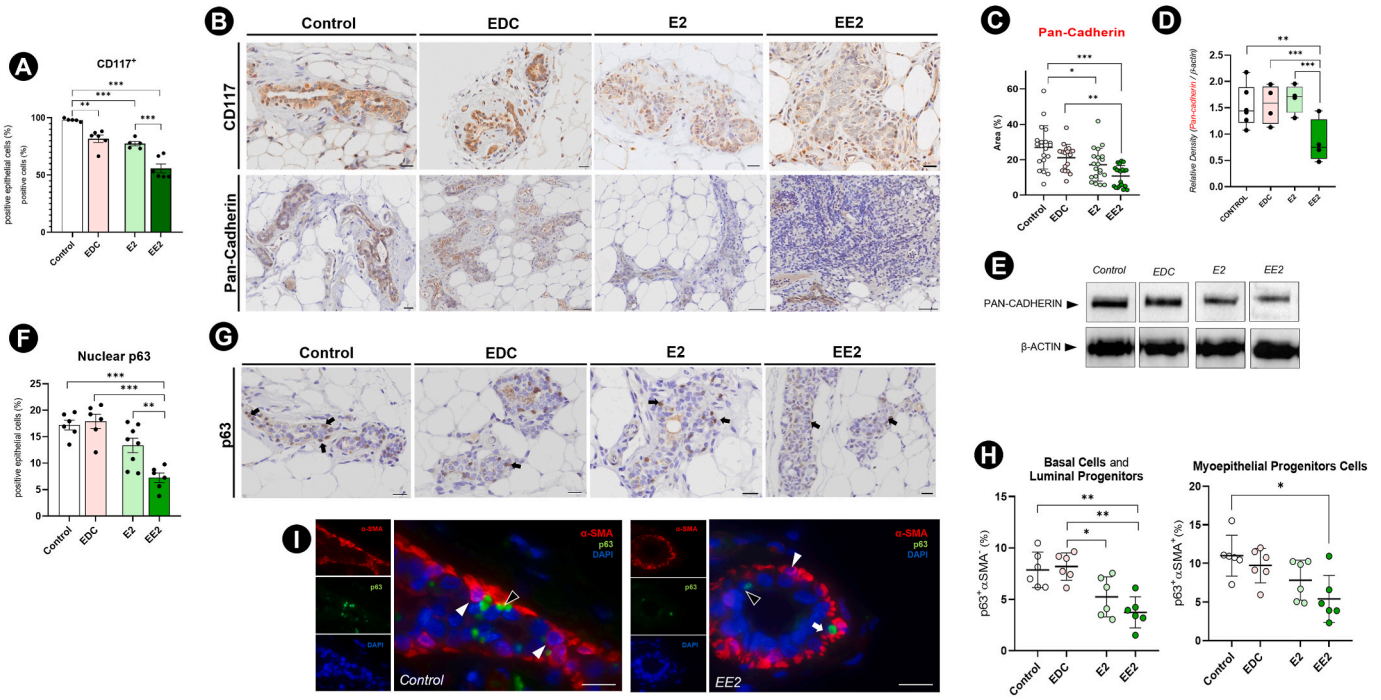

Fig. 2. Epithelial compartment characterization. **(A)** Quantification of CD117+ luminal cells. **(B)** Immunohistochemistry of CD117 and pan-cadherin expression. **(C)** Positive area percentage for pan-cadherin. **(D)** Relative protein density of pan-cadherin normalized to β-actin by Western blotting. **(E)** Representative Western blot bands. **(F–G)** Immunohistochemistry of total nuclear p63+ progenitor cells. **(H–I)** Double immunofluorescence images identifying basal (p63+α-SMA−) and myoepithelial (p63+α-SMA+) progenitor cells. Graphs in (H) represent a percentage of cells expressing p63 and αSMA. *Statistical representation* (*among groups*): $*P < 0.05$, $**P < 0.01$, and $***P < 0.001$. Scale Bars: (B) 20 μm; (G) 20 μm.

increased in *EE2*-exposed MG compared to other groups (Fig. 3E–F). However, BRCA1 expression did not present statistical differences among groups (Fig. 3E–F).

3.3. Proliferation and cell death indices under endocrine disruption-induced carcinogenesis and estrogenic therapy

Proliferation was evaluated by nuclear staining of PHH3. The percentage of proliferative cells was analyzed in the MG, and epithelial positive staining was considered (Fig. 4A–B). An increase in *E2* and *EE2*-exposed females was observed (Fig. 4A). Cell death index was evaluated by the expression of the final apoptotic cascade protein, caspase 3, in inactive/pro-caspase (pro-CASP3) and activated/cleaved (cleaved-CASP3) isoforms (Fig. 4C–D). The level of pro-CASP3 expression was slightly decreased in the EDC-treated group, whereas the control, E2, and EE2 groups showed comparable levels without significant differences among them (Fig. 4D). An imbalance was observed in the control group, with an increase in cleaved-CASP3 relative to pro-CASP3, suggesting increased apoptotic induction in MG of aged females. Only exposure to *EE2* promoted an anti-apoptotic imbalance, as evidenced by lower levels of cleaved-CASP3 than pro-CASP3 (Fig. 4C–D). Positive staining for both immunostainings in the control was observed in serial sections of the same region for caspase 3 isoforms (Fig. 4C).

WB analysis showed that the correlation between pro-CASP3 and cleaved-CASP3 modulated the cell death pathway when their levels were imbalanced. Pro-CASP3 was increased in all treatments exposed to BPA (EDC, E2, and EE2) (Fig. 4E–F), and cleaved-CASP3 decreased in these groups, compared to the control (Fig. 4E–F).

3.4. Hormone receptors expression

Immunohistochemical analysis revealed significant modulation of hormone receptor expression in the MG under endocrine-disrupting conditions and hormonal exposure (Fig. 5A). A marked increase in ERα expression was observed across all experimental groups (Fig. 5 B), suggesting an upregulation possibly triggered by exposure to the *EDC*. In contrast, ERβ expression was drastically reduced (Fig. 5C), with the *EE2*-treated group showing significantly lower expression than the *EDC* group. Progesterone receptor (PGR) expression also declined in all treated groups compared with the control, with E2 treatment resulting in a more pronounced reduction than *EE2* (Fig. 5D). HER2 expression did not differ significantly between the groups (Fig. 5E), suggesting limited sensitivity to the experimental treatments. For the androgen receptor (AR), an increase was observed in the EDC group compared to the control group; however, no significant differences were observed between the EE2 group and either the control or EDC groups, whereas E2 differed significantly from both *EDC* and *EE2* (Fig. 5F).

4. Discussion

In the present study, we evaluated the development of carcinogenesis in the mammary gland under three interacting perspectives: endocrine disruption, endocrine therapies, and aging. As far as we know, these scenarios have been explored separately in breast cancer research, but the association of factors is poorly understood. Estrogenic compounds used for endocrine therapies were able to promote carcinogenesis in MG of aged females under endocrine disruption by BPA during pregnancy and lactation, two critical windows of susceptibility for females (Terry et al., 2019; Rodgers et al., 2018). Previous studies from our research group indicated that the onset of carcinogenesis occurred with aging due to imbalances caused by exposure of mothers to BPA during pregnancy and lactation (Ruiz et al., 2021c, 2023b). A slight increase in *EDC*--treated females stated the onset of MG carcinogenesis. An important limitation of our study concerns the use of corn oil as the vehicle. Corn oil contains phytoestrogens; therefore, it is not biologically inert. Moreover, only BPA-exposed females received corn oil during the gestation-lactation window, and animals in the E2 and EE2 groups were exposed to corn oil again from twelve to eighteen months of age. This

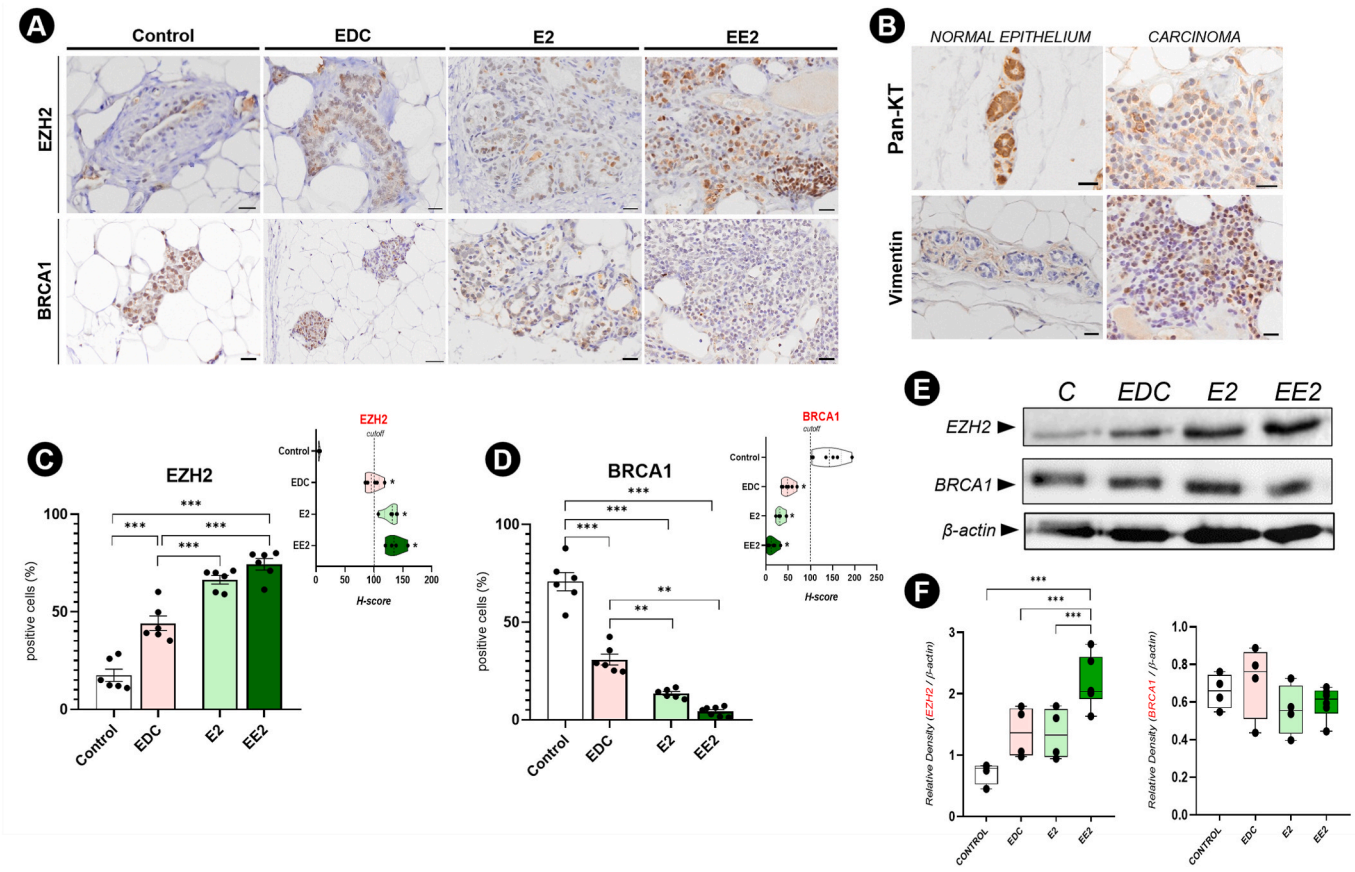

Fig. 3. EZH2 and BRCA1 expression in the MG. **(A)** Immunohistochemistry of EZH2 and BRCA1. **(B)** EMT characterization by pan-cytokeratin and vimentin co-expression. **(C)** Quantification and H-score of EZH2 expression. **(D)** Quantification and H-score of BRCA1 expression. **(E)** Western blot analysis of EZH2 and BRCA1 with relative density normalized to β-actin. *Statistical representation* (*among groups*): $*P < 0.05$, $**P < 0.01$, and $***P < 0.001$. *Scale Bars*: 20 μm.

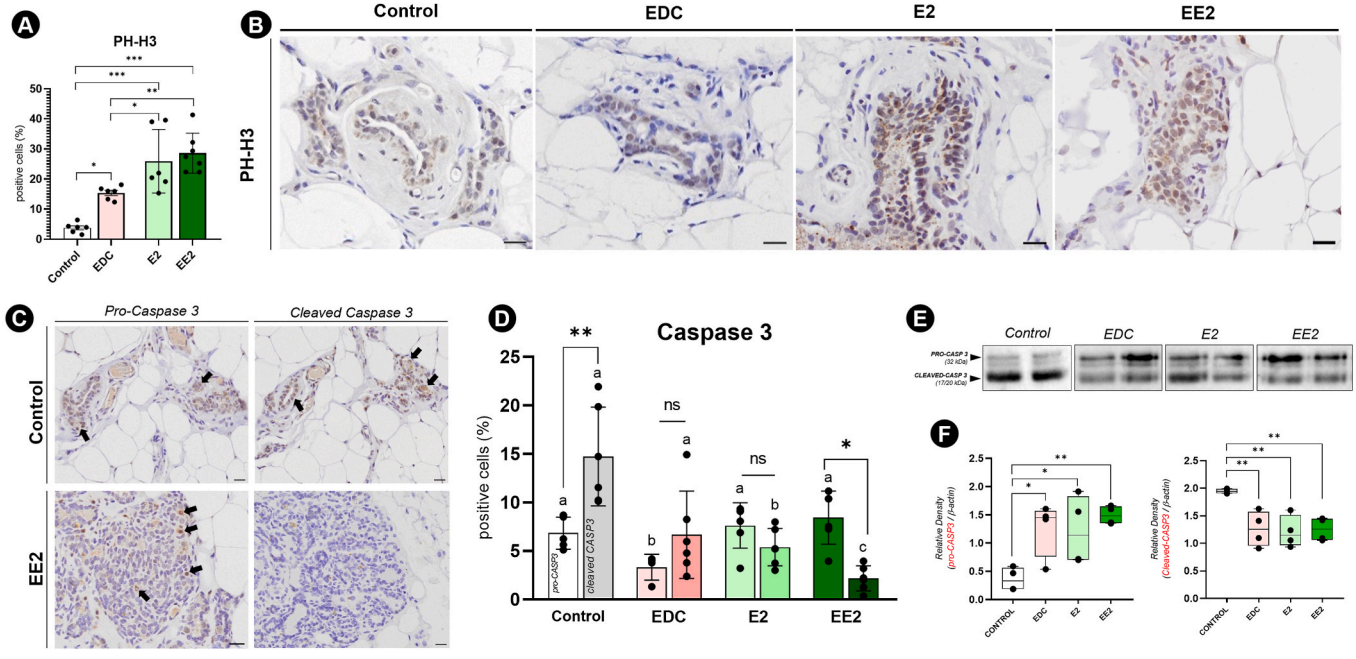

Fig. 4. Proliferation and apoptosis regulation. **(A–B)** PHH3 immunostaining as a marker of proliferation. **(C)** Immunohistochemistry for pro-caspase 3 and cleaved caspase 3 in control and EE2 groups. **(D)** Quantification of pro- and cleaved caspase 3-positive cells (arrows) across all groups. **(E)** Western blot bands for caspase 3 isoforms. **(F–G)** Densitometric quantification of pro-caspase 3 and cleaved caspase 3, respectively, normalized to β-actin. *Statistical representation* (*among groups*): $*P < 0.05$, $**P < 0.01$, and $***P < 0.001$. *Scale Bars*: 20 μm.

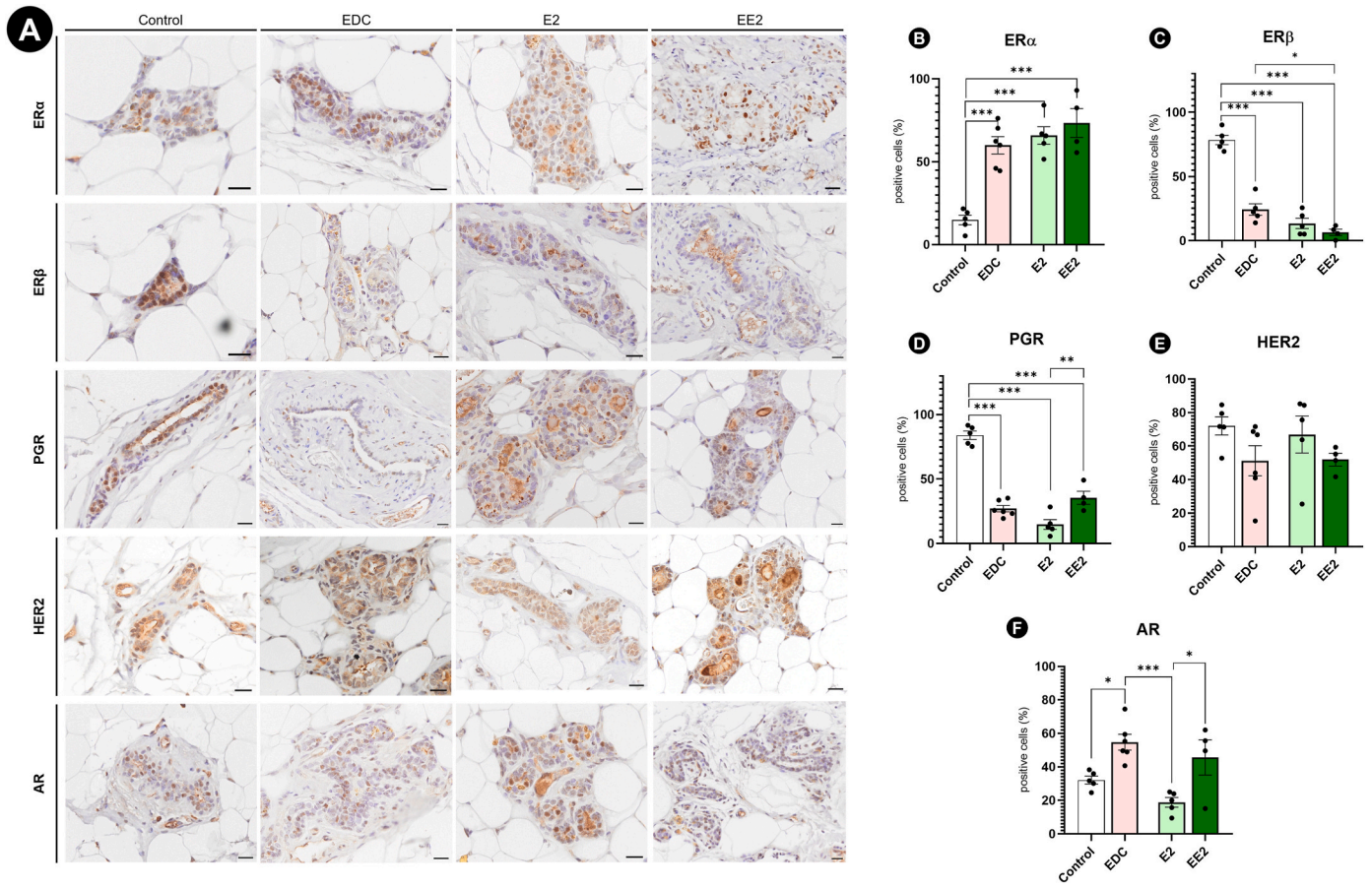

Fig. 5. Hormone receptor expression in mammary glands under endocrine disruption and estrogenic therapies. **(A)** Representative immunohistochemistry images of ERα, ERβ, PGR, HER2, and AR among control, EDC, E2, and EE2 groups. Scale bars: 20 μm. **(B–F)** Quantification of positively stained cells (% per field): **(B)** ERα was significantly upregulated in all treated groups. **(C)** ERβ expression was drastically reduced in E2 and EE2 groups, particularly under EE2. **(D)** PGR expression declined in all exposed groups, with a pronounced reduction under E2. **(E)** HER2 showed no significant differences among groups. **(F)** AR expression was elevated in the EDC group, whereas E2 treatment led to lower AR expression compared to EDC and EE2. *Statistical representation* (*among groups*): $^{*}P < 0.05$, $^{**}P < 0.01$, and $^{***}P < 0.001$. *Scale Bars*: 20 μm.

unequal vehicle exposure could introduce mild endocrine or metabolic influences and represents an additional lipid intake in those groups. Although our supplementary data show no significant differences in body weight or fat pad mass (Supplementary Table 1), these factors may still contribute to subtle effects on females. Future experiments will use a vehicle administered identically across all groups and will preferentially use oils with minimal estrogenic activity, thereby reducing potential confounding effects.

The development of tumoral features in MG was observed following estrogenic therapies, which induced a proliferative response and protective apoptotic machinery mediated by CASP3 in the epithelium, thereby allowing the progression of malignant and pre-malignant lesions. In addition, this imbalance affected the epithelial cell profile, leading to the loss of CD117+ luminal cells and a reduction in p63+ cells. Our data demonstrated the reorganization of the epithelial compartment following the induction of the EMT process, as evidenced by increased expression of the cancer marker EZH2 and decreased expression of BRCA1, and by the acquisition of mesenchymal features, such as the loss of cadherins. Our findings parallel human data linking hormone therapy to breast cancer risk. Clinical studies show that exogenous estrogens increase mammographic density (Ellingjord-Dale et al., 2014), a strong predictor of epithelial proliferation and cancer incidence. Similarly, estrogenic therapies in disrupted gerbil glands promoted epithelial lesions, altered receptor balance, and impaired apoptotic control. These results suggest that prior endocrine disruption may enhance tissue susceptibility to subsequent hormone exposure, underscoring the need to account for exposure history in menopausal therapy risk assessment.

Both estrogens used in the present study are relevant in hormonal replacement due to their action as an endogenous-similar (E2) and synthetic estrogen (EE2) (Stuenkel, 2015; De Leo et al., 2016). However, a pro-carcinogenic activity had already been assigned to both compounds under various conditions (Lobo, 2017; Hunter, 2017; Chen et al., 2006; Flores and Taylor, 2015). Aging is a critical period for menopause in females, in which a drastic decrease in serum estrogen happens, inducing an involution in the MG epithelium (Oh et al., 2016). Endocrine disruption, for example, with BPA exposure, characteristically changes this process, since it acts as a xenoestrogen and enhances neoplastic activity in MG (Soto et al., 2013; Acevedo et al., 2013). However, estrogen supplementation contributes to remodeling of branching density by inducing and reinforcing epithelial proliferation and lesion development. This effect is consistent with evidence that higher mammographic density reflects increased epithelial and stromal proliferation, which is strongly associated with elevated breast cancer risk (Azam et al., 2018). In agreement, experimental findings have shown that estrogens potentiate pre-existing epithelial alterations, such as hyperplastic foci, ductal carcinoma in situ (DCIS), and microinvasive carcinoma, thereby promoting the progression of early neoplastic changes (Itou et al., 2020). Although no palpable tumors were observed, histopathological and immunohistochemical analyses revealed epithelial lesions displaying neoplastic features consistent with DCIS or microinvasive carcinoma patterns, as defined in previous studies

(Makki, 2015; Hu et al., 2008; Lodillinsky et al., 2016; Zheng et al., 2014). Histological analysis allowed for the observation of the increase of hyperplasia and the occurrence of carcinoma, which are relevant grades for breast cancer diagnosis (Dall et al., 2018; Tawfik et al., 2007). These lesions were identified through disruption of the integrity of myoepithelial cells (α-SMA + cells) and loss of CD117 expression, which defines epithelial luminal cells (Kim and Villadsen, 2018). Micro-invasive carcinomas were increased in EE2 groups, whereas hyperplasia was predominant in E2-exposed females. Both lesions, malignant and pre-malignant, impair the functioning of MG beyond the installation of a tumoral process (Makki, 2015).

Remodeling of epithelial cell organization enables carcinogenesis, as these are the primary cells disrupted in breast cancer (Líška et al., 2016; Visvader and Stingl, 2014). Luminal cells are commonly associated with neoplastic activity due to their plasticity during reproductive cycles and their hormonal sensitization (Li et al., 2020b). Most luminal cells expressing CD117 and cytokeratin represent the proliferative population during homeostatic conditions in MG (Kim and Villadsen, 2018). Malignant mammary carcinoma shows decreased expression of CD117 (Schulmeyer et al., 2023). Besides high-grade carcinomas with EMT characteristics (Tsuda et al., 2005a, 2005b), reduced CD117 expression indicates a transition from in situ to differentiated carcinomas in histopathological analysis (Kondi-Pafiti et al., 2010). Our results demonstrated that a relative decrease in CD117+ luminal cells is associated with a diminishment of other epithelial cell types, probably due to EMT, which impairs the self-renewal of mammary epithelium (Zhao et al., 2021; Sikandar et al., 2017).

Progenitor cells, clustered by p63 positivity (Forster et al., 2014) originate from both main cell types of the epithelium: myoepithelial cells and luminal cells. In general, progenitor cells promote the ductal and alveolar epithelium identity (Visvader and Stingl, 2014), which is disrupted in cancer (Oakes et al., 2014). Neither myoepithelial progenitors ($p63n^{+}\alpha SMA^{+}$) nor basal/luminal progenitor ($p63n^{+}\alpha SMA^{-}$) cells were disrupted by BPA exposure, but estrogenic therapies led to a reduction in both populations, related to the loss of epithelial features (Forster et al., 2014). P63 is absent in metastatic phenotypes, associated with a decrease in the myoepithelial cell layer (Ding et al., 2019), which favors the invasiveness. Myoepithelial cells are responsible for the polarity of luminal cells since their contact with the basement membrane segregates the compartments (Ingthorsson et al., 2015; Gudjonsson et al., 2002; Man and Sang, 2004Man and Sang, 2004). The decrease in myoepithelial progenitor cell and basal/luminal progenitor cell numbers was expected due to the low number of progenitor cells for both populations. Corroborating this feature, BRCA1 expression is associated with the disruption of cells of the myoepithelial and basal lineage (Shalabi et al., 2021; Ding et al., 2019), which was decreased in both estrogenic therapies. This state affects the entire epithelial profile, as a proliferative disarray was assigned to this compartment in the present study. These associated events, with an inversion in the expression of distinctive markers for epithelium (pan-cytokeratin) and stroma (vimentin), indicate changes of EMT, which consequently disrupts polarity and epithelial unity.

Cadherins are calcium-dependent transmembrane proteins that promote the adhesion of cells (Son and Moon, 2013). E-cadherin is primarily in the luminal epithelial cells of MG (Dias et al., 2017), whereas P-cadherin is expressed by basal cells (Sirka et al., 2018). Pan-cadherin, a general marker, was expressed in MG exposed to estrogen therapies, with a significant decrease in EE2. This data corroborates the diminishment of normal epithelial cells and the increase of neoplastic cells in MG. Since estrogens are the main modulatory hormones of the epithelial layer (Cunha et al., 2004; Brisken and Ataca, 2015; Stingl, 2011), they generally promote increasing cell adhesion (Förster et al., 2002; Deng et al., 2020). Although estrogens can increase E-cadherin in ER-positive cancer cells (Maynadier et al., 2012; Bischoff et al., 2020), in our experiment, we observed that E2 reduced cadherin expression and favored microinvasive features in the mammary microenvironment previously exposed to BPA. This indicates that BPA-induced disruption modifies the epithelial response to estrogens and contributes to the establishment of a more invasive phenotype. For MG exposed to EE2, demonstrate that the decrease in pan-cadherin, followed in both morphological and molecular analyses, is related to an increased incidence of carcinoma phenotypes. Due to the impact of E-cadherin on the polarity of epithelium and tissue differentiation (Lee et al., 2017; Oral et al., 2016), the process that follows EE2 exposure could indicate a progression of EMT. The differences observed in the effects of estrogenic therapies and cadherin expression could be attributed to the dosing regimens applied, which were based on established therapeutic guidelines (Stuenkel et al., 2015; Ruggiero and Likis, 2002; De Leo et al., 2016) and to the differential receptor-binding affinities of the compounds (Merki-Feld et al., 2012; Escande et al., 2006; Cheverasan et al., 2018), which determine their relative potency in eliciting mammary gland responses. One aggravating factor is that exposure to BPA increases EMT with aging (Ruiz et al., 2021a; Wang et al., 2013), a differential effect observed in our study.

EMT is a critical factor in carcinoma development, and BPA exposure during the window of susceptibility in pregnancy and lactation contributes to this process as age progresses (Ruiz et al., 2021a). This process can be detected by the expression of mainly markers that demonstrate mutagenic changes associated with neoplastic development (Suriyamurthy et al., 2019; Katsuno et al., 2013). In the present work, we evaluated 2 of the main markers involved in EMT of the mammary gland, EZH2 and BRCA1 (Li et al., 2020a; Bai et al., 2022; Landragin et al., 2025). Our results allowed us to confirm that exposure to both estrogenic compounds led to the induction of this process through an inverse modulation of these two proteins. EZH2, a polycomb protein member of the methyltransferase of histone H3, acts as an activator of oncogenes linked to EMT (Li et al., 2020a; Adibfar et al., 2021). BRCA1 is one of the main histopathological markers for breast cancer, and its modulation is associated with mutagenic changes (V Fernandez et al., 2012; Mahmoud et al., 2017). Its reduction in tissues is related to severe tumor phenotypes (Shalabi et al., 2021) since it acts as a DNA repair protein (Thompson, 2010). The overmodulation under estrogenic treatment is reflected mainly in the histopathological diagnosis. EZH2 expression is primarily observed in hyperplastic foci and invasive carcinomas (Vougiouklakis et al., 2020; Li et al., 2009). BRCA1 decreasing indicates high histologic grade breast cancer (Hedau et al., 2015; Chang et al., 2022), as observed for the increased invasive microcarcinoma incidence in *E2* and *EE2*-treated females. It was reflected in the histological score (H-score) accessed by histopathological analysis, established for EZH2 and BRCA1 (Reid et al., 2021; Pierceall et al., 2011). Our study used values < 100 for EZH2 and >100 for BRCA1 as cutoffs for the H-score to indicate a free-neoplastic diagnosis, as previously employed (Vougiouklakis et al., 2020; Madjd et al., 2011). Both cancer markers showed a range distribution, indicating a generally poor prognosis for disrupted groups (Reid et al., 2021; Madjd et al., 2011). Notably, BPA exposure was a key factor in the expression of both markers, as no statistical differences were observed between the BPA-exposed and BPA plus estrogen-treated groups in the H-score analysis compared with the control. Thus, exposure to estrogenic compounds can use this machinery to increase tissue susceptibility and favor the transition to more aggressive and invasive phenotypes (Mahmoud et al., 2017; Mørch et al., 2017). Despite not presenting metastatic foci or palpable tumors, the MG of females exposed to both estrogenic compounds showed epithelial changes that favored a transition scenario.

Both endogenous and synthetic estrogens had the potential to negatively modulate tissue expression of BRCA1. This event, associated with exposure to BPA (Ruiz et al., 2021a), is unfavorable in an aging environment, making MG susceptible to tumor development (Raafat et al., 2012; Miyano et al., 2017). Estrogens promote cellular instabilities that require BRCA1 repair (Fan et al., 2001; Wang and Di, 2014), and its low expression indicates potential breast cancer

progression (Chang et al., 2022; Lambie et al., 2003). Estrogen-induced proliferation is mediated through the activation of downstream effectors, and BRCA1 serves as an essential modulator that suppresses ER–-driven transcription and limits proliferative signaling, thereby maintaining epithelial homeostasis (Wang and Di, 2014; Lamb et al., 2000). Since proliferative activity was enhanced by endocrine disruption and estrogenic therapies further boosted it, the investigation into imbalances in cell death also revealed damage to the apoptotic cascade. Caspase 3 is a key executor of apoptosis that keeps molecular pathways related to repair proteins in cancer (Pu et al., 2017; Asadi et al., 2022). EZH2 overexpression and BRCA1 downregulation alter cell fate, promoting the survival of cancerous cells (Puppe et al., 2019; Wang et al., 2021), as observed in the present work by diminishing caspase 3 activation. This phenomenon was observed in EE2 females, in which active-CASP3 was decreased relative to pro-CASP3. Contrarily, during perimenopause, as observed in the control group, MG is under involution due to low hormonal support (Martinson et al., 2013). Then, estrogenic therapies under endocrine disruption led to dysregulation of caspase 3 activation by cleavage, promoting an imbalance in proliferative index and aiding the increase of malignant lesions in MG.

Our data also demonstrated a distinct modulation of hormonal receptor expression profiles in MG exposed to *E2* and *EE2*. ERα expression was consistently elevated across all experimental groups, which aligns with previous observations of estrogenic overstimulation following BPA exposure and hormonal supplementation (Leonel et al., 2020b; Kanaya et al., 2019b). The PGR also decreased in all treated groups, with *E2* leading to a more severe reduction, corroborating findings that link ER/PR imbalance to proliferative lesions and lower differentiation potential (Dall et al., 2018). Interestingly, HER2 levels remained unaffected, suggesting limited responsiveness in this context. Furthermore, AR was increased only in the EDC group compared to the control group, while E2-treated females showed a significant decrease compared to EDC-treated females, reinforcing AR's context-dependent role in tumor progression (Cheung et al., 2003; Cunha et al., 2004; Tarulli et al., 2019). Together, these findings delineate a receptor-specific profile that may inform mechanistic insights into the differential carcinogenic potential of *E2* and *EE2* under endocrine disruption.

In summary, our results showed that both endogenous and synthetic estrogen therapies enhanced mammary gland carcinogenesis under conditions of endocrine disruption and aging. The main findings supporting tumor progression for both estrogenic compounds relate to imbalances in EZH2 and BRCA1 expressions, which affect proliferation and apoptotic balance. Remodeling of the epithelial cell profile led to a loss of CD117 luminal expression and reduced pan-cadherin expression, compromising compartment identity. In our model, endocrine-disrupted mammary glands that progressed from DCIS to invasive carcinoma also showed a reduction in $p63^{+}$ progenitor cells, which are known to sustain epithelial self-renewal (Boulevard, 2016). Similar findings have been reported in previous studies, in which loss of p63 was associated with disruption of the myoepithelial layer and the transition to invasive carcinoma (Hu et al., 2008; Lodillinsky et al., 2016). The high incidence of malignant lesions underscores the risk that estrogens pose for the development of breast cancer under endocrine disruption. Also, the hormone receptor profile induced by E2 and EE2, characterized by ERα upregulation and ERβ/PR suppression, reinforces the proliferative, apoptotic, and structural imbalances that lead to mammary carcinogenesis.

CRediT authorship contribution statement

Thalles Fernando Rocha Ruiz: Writing – original draft, Visualization, Validation, Project administration, Investigation, Formal analysis, Data curation, Conceptualization. **Stella Bicalho Silva:** Methodology, Investigation, Formal analysis. **Vitor Grigio:** Methodology, Investigation, Formal analysis. **Paula Rahal:** Validation, Funding acquisition. **Marília de Freitas Calmon:** Methodology, Funding acquisition, Formal analysis. **Patrícia Simone Leite Vilamaior:** Writing – original draft, Validation, Supervision, Project administration, Methodology, Conceptualization. **Ellen Cristina Rivas Leonel:** Writing – original draft, Visualization, Validation, Formal analysis, Data curation, Conceptualization. **Sebastião Roberto Taboga:** Writing – original draft, Visualization, Validation, Supervision, Funding acquisition, Conceptualization.

Funding

This study was supported by the São Paulo Research Foundation (FAPESP), grant numbers 2021/14140-5 (SRT) and 2022/00521-0 (TFRR); and supported by CNPq (National Council for Scientific and Technological Development), Brazil (grant number - 403028/2023-0).

Declaration of competing interest

The authors declare that they have no known competing financial interests or personal relationships that could have appeared to influence the work reported in this paper.

Acknowledgements

We express our sincere gratitude to the technical support of the MSC. Luiz Roberto Falleiros Junior and colleagues of Microscopy and Microanalysis Center (UNESP/IBILCE). Fundação de Amparo à Pesquisa financed this study do Estado de São Paulo (FAPESP) – Grant Numbers: 22/00521-0 (TFRR) and 21/14140-5 (SRT).

Appendix A. Supplementary data

Supplementary data to this article can be found online at https://doi.org/10.1016/j.mce.2025.112720.

Data availability

Data will be made available on request.

References

Acevedo, N., Davis, B., Schaeberle, C.M., Sonnenschein, C., Soto, A.M., 2013. Perinatally administered bisphenol A as a potential mammary gland carcinogen in RatsCorrection: a population-based case–control study of urinary arsenic species and squamous cell carcinoma in New Hampshire, USA. Environ. Health Perspect. 121, 1040–1046.

Adibfar, S., Elveny, M., Kashikova, H.S., Mikhailova, M.V., Farhangnia, P., Vakili-Samiani, S., Tarokhian, H., Jadidi-Niaragh, F., 2021. The molecular mechanisms and therapeutic potential of EZH2 in breast cancer. Life Sci. 286, 120047. https://doi.org/10.1016/j.lfs.2021.120047.

Asadi, M., Taghizadeh, S., Kaviani, E., Vakili, O., Taheri-Anganeh, M., Tahamtan, M., Savardashtaki, A., 2022. Caspase-3: structure, function, and biotechnological aspects. Biotechnol. Appl. Biochem. 69, 1633–1645. https://doi.org/10.1002/bab.2233.

Atlas, E., Dimitrova, V., 2019. Bisphenol S and bisphenol A disrupt morphogenesis of MCF-12A human mammary epithelial cells. Sci. Rep. 9, 1–10. https://doi.org/10.1038/s41598-019-52505-x.

Azam, S., Lange, T., Huynh, S., Aro, A.R., von Euler-Chelpin, M., Vejborg, I., Tjønneland, A., Lynge, E., Andersen, Z.J., 2018. Hormone replacement therapy, mammographic density, and breast cancer risk: a cohort study. Cancer Causes Control 29, 495–505. https://doi.org/10.1007/s10552-018-1033-0.

Bai, F., Wang, C., Liu, X., Hollern, D., Liu, S., Fan, C., Liu, C., Ren, S., Herschkowitz, J.I., Zhu, W.G., Pei, X.H., 2022. Loss of function of BRCA1 promotes EMT in mammary tumors through activation of TGFβR2 signaling pathway. Cell Death Dis. 13, 1–13. https://doi.org/10.1038/s41419-022-04646-7.

Bhan, A., Hussain, I., Ansari, K.I., Bobzean, S.A.M., Perrotti, L.I., Mandal, S.S., 2014. Histone methyltransferase EZH2 is transcriptionally induced by estradiol as well as estrogenic endocrine disruptors bisphenol-a and diethylstilbestrol. J. Mol. Biol. 426, 3426–3441. https://doi.org/10.1016/j.jmb.2014.07.025.

Biondi, L.R., Tedardi, M.V., Gentile, L.B., Chamas, P.P.C., Dagli, M.L.Z., 2021. Quantification of global DNA methylation in canine mammary gland tumors via immunostaining of 5-Methylcytosine: histopathological and clinical correlations. Front. Vet. Sci. 8, 1–13. https://doi.org/10.3389/fvets.2021.628241.

Bischoff, P., Kornhuber, M., Dunst, S., Zell, J., Fauler, B., Mielke, T., Taubenberger, A.V., Guck, J., Oelgeschläger, M., Schönfelder, G., 2020. Estrogens determine adherens

junction organization and E-Cadherin clustering in breast cancer cells via amphiregulin. iScience 23. https://doi.org/10.1016/j.isci.2020.101683.
Bleak, T.C., Calaf, G.M., 2021. Breast and prostate glands affected by environmental substances. Oncol. Rep. 45, 1–18. https://doi.org/10.3892/or.2021.7971 (Review).
Boulevard, W.U., 2016. p63 role in breast cancer simone. Aging (Albany. NY) 8, 2256–2257. https://doi.org/10.1111/j.1749.
Brisken, C., Ataca, D., 2015. Endocrine hormones and local signals during the development of the mouse mammary gland. Wiley Interdiscip. Rev. Dev. Biol. 4, 181–195. https://doi.org/10.1002/wdev.172.
Buteau-Lozano, H., Velasco, G., Cristofari, M., Balaguer, P., Perrot-Applanat, M., 2008. Xenoestrogens modulate vascular endothelial growth factor secretion in breast cancer cells through an estrogen receptor-dependent mechanism. J. Endocrinol. 196, 399–412. https://doi.org/10.1677/JOE-07-0198.
Butler, L., Santoro, N., 2011. The reproductive endocrinology of the menopausal transition. Steroids 76, 627–635. https://doi.org/10.1016/j.steroids.2011.02.026.
Chang, H.J., Yang, U.C., Lai, M.Y., Chen, C.H., Fann, Y.C., 2022. High BRCA1 gene expression increases the risk of early distant metastasis in ER+ breast cancers. Sci. Rep. 12, 1–13. https://doi.org/10.1038/s41598-021-03471-w.
Chen, W.Y., Manson, J.A.E., Hankinson, S.E., Rosner, B., Holmes, M.D., Willett, W.C., Colditz, G.A., 2006. Unopposed estrogen therapy and the risk of invasive breast cancer. Arch. Intern. Med. 166, 1027–1032. https://doi.org/10.1049/el:20061631.
Cheung, S.Y., Yuen, M.T., Choi, H.L., Cheng, H.K., Huang, Y., Chen, S., Chan, F.L., 2003. An expression study of hormone receptors in spontaneously developed, carcinogen-induced and hormone-induced mammary tumors in female noble rats. Int. J. Oncol. 22, 1383–1395. https://doi.org/10.3892/ijo.22.6.1383.
Cheverasan, A., Mioc, M., Simu, S., Soica, C., Dehelean, C., Szasz, F., Navolan, D., Poenaru, M., 2018. Binding affinity of 17-β-ethinylestradiol to normal and mutant types of estrogen receptors: an in silico evaluation. Rev. Chim. 69, 2067–2070. https://doi.org/10.37358/rc.18.8.6475.
Cho, K.H., Jeong, B.Y., Park, C.G., Lee, H.Y., 2019. The YB-1/EZH2/amphiregulin signaling axis mediates LPA-induced breast cancer cell invasion. Arch Pharm. Res. (Seoul) 42, 519–530. https://doi.org/10.1007/s12272-019-01149-6.
Corrales, J., Kristofco, L.A., Steele, W.B., Yates, B.S., Breed, C.S., Williams, E.S., Brooks, B.W., 2015. Global assessment of bisphenol A in the environment: review and analysis of its occurrence and bioaccumulation. Dose Response 13, 1559325815598308. https://doi.org/10.1177/1559325815598308.
Cunha, G.R., Cooke, P.S., Kurita, T., 2004. Role of stromal-epithelial interactions in hormonal responses. Arch. Histol. Cytol. 67, 417–434. https://doi.org/10.1679/aohc.67.417.
Dall, G.V., Hawthorne, S., Seyed-Razavi, Y., Vieusseux, J., Wu, W., Gustafsson, J.A., Byrne, D., Murphy, L., Risbridger, G.P., Britt, K.L., 2018. Estrogen receptor subtypes dictate the proliferative nature of the mammary gland. J. Endocrinol. 237, 323–336. https://doi.org/10.1530/JOE-17-0582.
Dawson, C.A., Visvader, J.E., 2021. The cellular organization of the mammary gland: insights from microscopy. J. Mammary Gland Biol. Neoplasia. https://doi.org/10.1007/s10911-021-09483-6.
De Leo, V., Musacchio, M.C., Cappelli, V., Piomboni, P., Morgante, G., 2016. Hormonal contraceptives: pharmacology tailored to women's health. Hum. Reprod. Update 22, 634–646. https://doi.org/10.1093/humupd/dmw016.
Del Pup, L., Codacci-Pisanelli, G., Peccatori, F., 2019. Breast cancer risk of hormonal contraception: counselling considering new evidence. Crit. Rev. Oncol. Hematol. 137, 123–130. https://doi.org/10.1016/j.critrevonc.2019.03.001.
Deng, Y., Miki, Y., Nakanishi, A., 2020. Estradiol/GPER affects the integrity of mammary duct-like structures in vitro. Sci. Rep. 10, 1–15. https://doi.org/10.1038/s41598-020-57819-9.
Dias, K., Dvorkin-Gheva, A., Hallett, R.M., Wu, Y., Hassell, J., Pond, G.R., Levine, M., Whelan, T., Bane, A.L., 2017. Claudin-low breast cancer; clinical & pathological characteristics. PLoS One 12, 1–17. https://doi.org/10.1371/journal.pone.0168669.
Ding, L., Su, Y., Fassl, A., Hinohara, K., Qiu, X., Harper, N.W., Huh, S.J., Bloushtain-Qimron, N., Jovanović, B., Ekram, M., Zi, X., Hines, W.C., Alečković, M., Gil del Alcazar, C., Caulfield, R.J., Bonal, D.M., De Nguyen, Q., Merino, V.F., Choudhury, S., Ethington, G., Panos, L., Grant, M., Herlihy, W., Au, A., Rosson, G.D., Argani, P., Richardson, A.L., Dillon, D., Allred, D.C., Babski, K., Kim, E.M.H., McDonnell, C.H., Wagner, J., Rowberry, R., Bobolis, K., Kleer, C.G., Hwang, E.S., Blum, J.L., Cristea, S., Sicinski, P., Fan, R., Long, H.W., Sukumar, S., Yeon Park, S., Garber, J.E., Bissell, M., Yao, J., Polyak, K., 2019. Perturbed myoepithelial cell differentiation in BRCA mutation carriers and in ductal carcinoma in situ. Nat. Commun. 10, 1–16. https://doi.org/10.1038/s41467-019-12125-5.
Doshi, T., Mehta, S.S., Dighe, V., Balasinor, N., Vanage, G., 2011. Hypermethylation of estrogen receptor promoter region in adult testis of rats exposed neonatally to bisphenol A. Toxicology 289, 74–82. https://doi.org/10.1016/j.tox.2011.07.011.
Duivenvoorden, H.M., Spurling, A., O'Toole, S.A., Parker, B.S., 2018. Discriminating the earliest stages of mammary carcinoma using myoepithelial and proliferative markers. PLoS One 13, 1–12. https://doi.org/10.1371/journal.pone.0201370.
Dumitrascu, M., Mares, C., Petca, R.-C., Sandru, F., Popescu, R.-I., Mehedintu, C., Petca, A., 2020. Carcinogenic effects of bisphenol A in breast and ovarian cancers. Oncol. Lett. 20. https://doi.org/10.3892/ol.2020.12145 (Review).
Ellingjord-Dale, M., Grotmol, T., Lee, E., Van Den Berg, D.J., Hofvind, S., Couto, E., Sovio, U., Dos-Santos-Silva, I., Ursin, G., 2014. Breast cancer susceptibility variants and mammographic density phenotypes in norwegian postmenopausal women. Cancer Epidemiol. Biomarkers Prev. 23, 1752–1763. https://doi.org/10.1158/1055-9965.EPI-13-1212.
Escande, A., Pillon, A., Servant, N., Cravedi, J.P., Larrea, F., Muhn, P., Nicolas, J.C., Cavaillès, V., Balaguer, P., 2006. Evaluation of ligand selectivity using reporter cell lines stably expressing estrogen receptor alpha or beta. Biochem. Pharmacol. 71, 1459–1469. https://doi.org/10.1016/j.bcp.2006.02.002.
Fan, S., Ma, Y.X., Wang, C., Yuan, R.Q., Meng, Q., Wang, J.A., Erdos, M., Goldberg, I.D., Webb, P., Kushner, P.J., Pestell, R.G., Rosen, E.M., 2001. Role of direct interaction in BRCA1 inhibition of estrogen receptor activity. Oncogene 20, 77–87. https://doi.org/10.1038/sj.onc.1204073.
Fernandez, S.V., Russo, J., 2010. Estrogen and xenoestrogens in breast cancer. Toxicol. Pathol. 38, 110–122. https://doi.org/10.1177/0192623309354108.
Flores, V.A., Taylor, H.S., 2015. The effect of menopausal hormone therapies on breast cancer. Avoiding the risk. Endocrinol. Metab. Clin. North Am. 44, 587–602. https://doi.org/10.1016/j.ecl.2015.05.007.
Förster, C., Mäkela, S., Wärri, A., Kietz, S., Becker, D., Hultenby, K., Warner, M., Gustafsson, J.Å., 2002. Involvement of estrogen receptor β in terminal differentiation of mammary gland epithelium. Proc. Natl. Acad. Sci. U. S. A 99, 15578–15583. https://doi.org/10.1073/pnas.192561299.
Forster, N., Saladi, S.V., vanBragt, M., Sfondouris, M.E., Jones, F.E., Li, Z., Ellisen, L.W., 2014. Basal cell signaling by p63 controls luminal progenitor function and lactation via NRG1. Dev. Cell 28, 147–160. https://doi.org/10.1016/j.devcel.2013.11.019.
Freneaux, P., Stoppa-Lyonnet, D., Mouret, E., Kambouchner, M., Nicolas, A., Zafrani, B., Vincent-Salomon, A., Fourquet, A., Magdelenat, H., Sastre-Garau, X., 2000. Low expression of bcl-2 in Brca1-associated breast cancers. Br. J. Cancer 83, 1318–1322. https://doi.org/10.1054/bjoc.2000.1438.
Gagniac, L., Rusidzé, M., Boudou, F., Cagnet, S., Adlanmerini, M., Jeannot, P., Gaide, N., Giton, F., Besson, A., Weyl, A., Gourdy, P., Raymond-Letron, I., Arnal, J.F., Brisken, C., Lenfant, F., 2020. Membrane expression of the estrogen receptor ERα is required for intercellular communications in the mammary epithelium. Dev 147. https://doi.org/10.1242/dev.182303.
Gomez, A.L., Delconte, M.B., Altamirano, G.A., Vigezzi, L., Bosquiazzo, V.L., Barbisan, L. F., Ramos, J.G., Luque, E.H., Muñoz-de-Toro, M., Kass, L., 2017. Perinatal exposure to bisphenol A or diethylstilbestrol increases the susceptibility to develop mammary gland lesions after estrogen replacement therapy in middle-aged rats, horm. Cancer. 8, 78–89. https://doi.org/10.1007/s12672-016-0282-1.
Gudjonsson, T., Rønnov-jessen, L., Villadsen, R., Rank, F., Mina, J., Petersen, O.W., 2002. Normal and tumor-derived myoepithelial cells differ in their ability to interact with luminal breast epithelial cells for polarity and basement membrane deposition. J. Cell Sci. 115, 39–50.
Hedau, S., Batra, M., Singh, U.R., Bharti, A.C., Ray, A., Das, B.C., 2015. Expression of BRCA1 and BRCA2 proteins and their correlation with clinical staging in breast cancer. J. Cancer Res. Ther. 11, 158–163. https://doi.org/10.4103/0973-1482.140985.
Hodis, H.N., Mack, W.J., Henderson, V.W., Shoupe, D., Budoff, M.J., Hwang-Levine, J., Li, Y., Feng, M., Dustin, L., Kono, N., Stanczyk, F.Z., Selzer, R.H., Azen, S.P., 2016. Vascular effects of early versus late postmenopausal treatment with estradiol. N. Engl. J. Med. 374, 1221–1231. https://doi.org/10.1056/NEJMoa1505241.
Hu, M., Yao, J., Carroll, D.K., Weremowicz, S., Chen, H., Carrasco, D., Richardson, A., Violette, S., Nikolskaya, T., Nikolsky, Y., Bauerlein, E.L., Hahn, W.C., Gelman, R.S., Allred, C., Bissell, M.J., Schnitt, S., Polyak, K., 2008. Regulation of in situ to invasive breast carcinoma transition. Cancer Cell 13, 394–406. https://doi.org/10.1016/j.ccr.2008.03.007.
Hunter, D.J., 2017. Oral contraceptives and the small increased risk of breast cancer. N. Engl. J. Med. 377, 2276–2277. https://doi.org/10.1056/nejme1709636.
Ingthorsson, S., Hilmarsdottir, B., Kricker, J., Magnusson, M.K., Gudjonsson, T., 2015. Context-dependent function of myoepithelial cells in breast morphogenesis and neoplasia. Curr. Mol. Biol. Reports 1, 168–174. https://doi.org/10.1007/s40610-015-0027-x.
Inman, J.L., Robertson, C., Mott, J.D., Bissell, M.J., 2015. Mammary gland development: cell fate specification, stem cells and the microenvironment. Dev 142, 1028–1042. https://doi.org/10.1242/dev.087643.
Itou, J., Takahashi, R., Sasanuma, H., Tsuda, M., Morimoto, S., Matsumoto, Y., Ishii, T., Sato, F., Takeda, S., Toi, M., 2020. Estrogen induces mammary ductal dysplasia via the upregulation of myc expression in a DNA-Repair-Deficient condition. iScience 23, 100821. https://doi.org/10.1016/j.isci.2020.100821.
Kanaya, N., Chang, G., Wu, X., Saeki, K., Bernal, L., Shim, H.-J., Wang, J., Warden, C., Yamamoto, T., Li, J., Park, J.-S., Synold, T., Vonderfecht, S., Rakoff, M., Neuhausen, S.L., Chen, S., 2019a. Single-cell RNA-Sequencing analysis of estrogen- and endocrine-disrupting chemical-induced reorganization of mouse mammary gland. Commun. Biol. 2, 406. https://doi.org/10.1038/s42003-019-0618-9.
Kanaya, N., Chang, G., Wu, X., Saeki, K., Bernal, L., Shim, H.-J., Wang, J., Warden, C., Yamamoto, T., Li, J., Park, J.-S., Synold, T., Vonderfecht, S., Rakoff, M., Neuhausen, S.L., Chen, S., Dasari, P., Sharkey, D.J., Noordin, E., Glynn, D.J., Hodson, L.J., Chin, P.Y., Evdokiou, A., Robertson, S.A., Ingman, W.V., Allavena, P., Sica, A., Solinas, G., Porta, C., Mantovani, A., Aoki, M., Pawankar, R., Niimi, Y., Kawana, S., Clark, N.M., Bos, P.D., Clarkson, R.W.E., Boland, M.P., Kritikou, E.A., Lee, J.M., Freeman, T.C., Tiffen, P.G., Watson, C.J., Dawson, C.A., Pal, B., Vaillant, F., Gandolfo, L.C., Liu, Z., Bleriot, C., Ginhoux, F., Smyth, G.K., Lindeman, G.J., Mueller, S.N., Rios, A.C., Visvader, J.E., Durando, M., Kass, L., Piva, J., Sonnenschein, C., Soto, A.M., Luque, E.H., Muñoz-De-Toro, M., Elgert, K.D., Alleva, D.G., Mullins, D.W., Gan, L., Qiu, Z., Huang, J.J., Li, Y., Huang, H., Xiang, T., Wan, J., Hui, T., Lin, Y., Li, H., Ren, G., Huang, F.M., Chang, Y.C., Lee, S.S., Yang, M. L., Kuan, Y.H., Mendes, L.O., Amorim, J.P.A., Teixeira, G.R., Chuffa, L.G.A., Fioruci, B.A., Pimentel, T.A., de Mello, W., Padovani, C.R., Pereira, S., Martinez, M., Pinheiro, P.F.F., Oliani, S.M., Martinez, F.E., Kupferman, M.E., Fini, M.E., Muller, W. J., Weber, R., Cheng, Y., Muschel, R.J., Lilla, J.N., Joshi, R.V., Craik, C.S., Werb, Z., Liu, Y., Mei, C., Liu, H., Wang, H., Zeng, G., Lin, J., Xu, M., Pollard, Jeffrey W., Ramírez-Valadez, K.A., Vázquez-Victorio, G., Macías-Silva, M., González-Espinosa, C., Van Dang, H., Sakai, T., Pham, T.A., Tran, D.H., Yorita, K., Shishido, Y., Fukui, K., Stein, T., Morris, J.S., Davies, C.R., Weber-Hall, S.J., Duffy, M.A., Heath, V. J., Bell, A.K., Ferrier, R.K., Sandilands, G.P., Gusterson, B.A., Ungari, M., Ferrero, G.,

Varotti, E., Gusolfino, M.D., Manotti, L., Tanzi, G., Trombatore, M., Bertoni, R., Wani, N.A., Nasser, M.W., Ahirwar, D.K., Zhao, H., Miao, Z., Shilo, K., Ganju, R.K., Yang, L., Huang, J.J., Ren, X., Gorska, A.E., Chytil, A., Aakre, M., Carbone, D.P., Matrisian, L.M.M., Richmond, A., Lin, P.C., Moses, H.L., Zollo, M., Di Dato, V., Spano, D., De Martino, D., Liguori, L., Marino, N., Vastolo, V., Navas, L., Garrone, B., Mangano, G., Biondi, G., Guglielmotti, A., 2019b. Single-cell RNA-sequencing analysis of estrogen- and endocrine-disrupting chemical-induced reorganization of mouse mammary gland. J. Biol. Chem. 66, 406. https://doi.org/10.1038/s42003-019-0618-9.

Katsuno, Y., Lamouille, S., Derynck, R., 2013. TGF-β signaling and epithelial-mesenchymal transition in cancer progression. Curr. Opin. Oncol. 25, 76–84. https://doi.org/10.1097/CCO.0b013e32835b6371.

Khan, N.G., Correia, J., Adiga, D., Rai, P.S., Dsouza, H.S., Chakrabarty, S., Kabekkodu, S. P., 2021. A comprehensive review on the carcinogenic potential of bisphenol A: clues and evidence. Environ. Sci. Pollut. Res. 28, 19643–19663. https://doi.org/10.1007/s11356-021-13071-w.

Kim, J., Villadsen, R., 2018. Expression of luminal progenitor marker CD117 in the human breast gland. J. Histochem. Cytochem. 66, 879–888. https://doi.org/10.1369/0022155418788845.

Kondi-Pafiti, A., Arkadopoulos, N., Gennatas, C., Michalaki, V., Frangou-Plegmenou, M., Chatzipantelis, P., 2010. Expression of c-kit in common benign and malignant breast lesions. Tumori 96, 978–984. https://doi.org/10.1177/548.6519.

Lamb, J., Ladha, M.H., McMahon, C., Sutherland, R.L., Ewen, M.E., 2000. Regulation of the functional interaction between cyclin D1 and the estrogen receptor. Mol. Cell Biol. 20, 8667–8675. https://doi.org/10.1128/mcb.20.23.8667-8675.2000.

Lambie, H., Miremadi, A., Pinder, S.E., Bell, J.A., Wencyk, P., Paish, E.C., Macmillan, R. D., Ellis, I.O., 2003. Prognostic significance of BRCA1 expression in sporadic breast carcinomas. J. Pathol. 200, 207–213. https://doi.org/10.1002/path.1348.

Landragin, C., Saichi, M., Laisné, M., Durand, A., Prompsy, P., Leclere, R., Mesple, J., Borgman, K., Trouchet, A., Faraldo, M.M., Chiche, A., Vincent-Salomon, A., Salmon, H., Vallot, C., 2025. Epigenomic disorder and partial EMT impair luminal progenitor integrity in Brca1-associated breast tumorigenesis. Mol. Cancer 24. https://doi.org/10.1186/s12943-025-02331-9.

Lee, H.M., Hwang, K.A., Choi, K.C., 2017. Diverse pathways of epithelial mesenchymal transition related with cancer progression and metastasis and potential effects of endocrine disrupting chemicals on epithelial mesenchymal transition process. Mol. Cell. Endocrinol. 457, 103–113. https://doi.org/10.1016/j.mce.2016.12.026.

Leonel, E.C.R., Campos, S.G.P., Bedolo, C.M.B., Guerra, L.H.A., Vilamaior, P.S.L., Calmon, M.F., Rahal, P., Amorim, C.A., Taboga, S.R., 2020a. Perinatal exposure to bisphenol A impacts in the mammary gland morphology of adult Mongolian gerbils. Exp. Mol. Pathol. 113, 104374. https://doi.org/10.1016/j.yexmp.2020.104374.

Leonel, E.C.R., Campos, S.G.P., Guerra, L.H.A., Bedolo, C.M., Vilamaior, P.S.L., Calmon, M.F., Rahal, P., Amorim, C.A., Taboga, S.R., 2020b. Impact of perinatal bisphenol A and 17β estradiol exposure: comparing hormone receptor response. Ecotoxicol. Environ. Saf. 188, 109918. https://doi.org/10.1016/j.ecoenv.2019.109918.

Leonel, E.C.R., Campos, S.G.P., Bedolo, C.M.B., Guerra, L.H.A., Vilamaior, P.S.L., Calmon, M.F., Rahal, P., Amorim, C.A., Taboga, S.R., 2020c. Perinatal exposure to bisphenol A impacts in the mammary gland morphology of adult Mongolian gerbils. Exp. Mol. Pathol. 113, 104374. https://doi.org/10.1016/j.yexmp.2020.104374.

Li, X., Gonzalez, M.E., Toy, K., Filzen, T., Merajver, S.D., Kleer, C.G., 2009. Targeted overexpression of EZH2 in the mammary gland disrupts ductal morphogenesis and causes epithelial hyperplasia. Am. J. Pathol. 175, 1246–1254. https://doi.org/10.2353/ajpath.2009.090042.

Li, Z., Wang, D., Lu, J., Huang, B., Wang, Y., Dong, M., Fan, D., Li, H., Gao, Y., Hou, P., Li, M., Liu, H., Pan, Z.Q., Zheng, J., Bai, J., 2020a. Methylation of EZH2 by PRMT1 regulates its stability and promotes breast cancer metastasis. Cell Death Differ. 27, 3226–3242. https://doi.org/10.1038/s41418-020-00615-9.

Li, C.M.C., Shapiro, H., Tsiobikas, C., Selfors, L.M., Chen, H., Rosenbluth, J., Moore, K., Gupta, K.P., Gray, G.K., Oren, Y., Steinbaugh, M.J., Guerriero, J.L., Pinello, L., Regev, A., Brugge, J.S., 2020b. Aging-associated alterations in mammary epithelia and stroma revealed by single-cell RNA sequencing. Cell Rep. 33, 108566. https://doi.org/10.1016/j.celrep.2020.108566.

Liao, D.Z.J., Pantazis, C.G., Hou, X., Li, S.A., 1998. Promotion of estrogen-induced mammary gland carcinogenesis by androgen in the male noble rat: probable mediation by steroid receptors. Carcinogenesis 19, 2173–2180. https://doi.org/10.1093/carcin/19.12.2173.

Líška, J., Brtko, J., Dubovický, M., Macejová, D., Kissová, V., Polák, Š., Ujházy, E., 2016. Relationship between histology, development and tumorigenesis of mammary gland in female rat. Exp. Anim. 65, 1–9. https://doi.org/10.1538/expanim.15-0055.

Lobo, R.A., 2017. Hormone-replacement therapy: current thinking. Nat. Rev. Endocrinol. 13, 220–231. https://doi.org/10.1038/nrendo.2016.164.

Lodillinsky, C., Infante, E., Guichard, A., Chaligné, R., Fuhrmann, L., Cyrta, J., Irondelle, M., Lagoutte, E., Vacher, S., Bonsang-Kitzis, H., Glukhova, M., Reyal, F., Bièche, I., Vincent-Salomon, A., Chavrier, P., 2016. p63/MT1-MMP axis is required for in situ to invasive transition in basal-like breast cancer. Oncogene 35, 344–357. https://doi.org/10.1038/onc.2015.87.

Madjd, Z., Karimi, A., Molanae, S., Asadi-Lari, M., 2011. BRCA1 protein expression level and CD44+ phenotype in breast cancer patients. Cell J. 13, 155–162.

Mahmoud, A.M., Macias, V., Al-alem, U., Deaton, R.J., Kadjaksy-Balla, A., Gann, P.H., Rauscher, G.H., 2017. BRCA1 protein expression and subcellular localization in primary breast cancer: automated digital microscopy analysis of tissue microarrays. PLoS One 12, 1–24. https://doi.org/10.1371/journal.pone.0184385.

Makki, J., 2015. Diversity of breast carcinoma: histological subtypes and clinical relevance. Clin. Med. Insights Pathol. 8, 23–31. https://doi.org/10.4137/CPath.s31563.

Mallepell, S., Krust, A., Chambon, P., Brisken, C., 2006. Paracrine signaling through the epithelial estrogen receptor α is required for proliferation and morphogenesis in the mammary gland. Proc. Natl. Acad. Sci. U. S. A 103, 2196–2201. https://doi.org/10.1073/pnas.0510974103.

Man, Y.G., Sang, Q.X.A., 2004. The significance of focal myoepithelial cell layer disruptions in human breast tumor invasion: a paradigm shift from the "protease-centered" hypothesis. Exp. Cell Res. 301, 103–118. https://doi.org/10.1016/j.yexcr.2004.08.037.

Marchese, S., Silva, E., 2012. Disruption of 3D MCF-12A breast cell cultures by estrogens - an In vitro model for ER-Mediated changes indicative of hormonal carcinogenesis. PLoS One 7, 1–11. https://doi.org/10.1371/journal.pone.0045767.

Martinson, H.A., Lyons, T.R., Giles, E.D., Borges, V.F., Schedin, P., 2013. Developmental windows of breast cancer risk provide opportunities for targeted chemoprevention. Exp. Cell Res. 319, 1671–1678. https://doi.org/10.1016/j.yexcr.2013.04.018.

Maynadier, M., Chambon, M., Basile, I., Gleizes, M., Nirde, P., Gary-Bobo, M., Garcia, M., 2012. Estrogens promote cell-cell adhesion of normal and malignant mammary cells through increased desmosome formation. Mol. Cell. Endocrinol. 364, 126–133. https://doi.org/10.1016/j.mce.2012.08.016.

McCave, E.J., Cass, C.A.P., Burg, K.J.L., Booth, B.W., 2010. The normal microenvironment directs mammary gland development. J. Mammary Gland Biol. Neoplasia 15, 291–299. https://doi.org/10.1007/s10911-010-9190-0.

Merki-Feld, G.S., Seeger, H., Mueck, A.O., 2012. Proliferative effects of estradiol- or ethinylestradiol-progestogen combinations on human breast cancer cells in an intermitted and a long-term regimen. Horm. Metab. Res. 44, 415–421. https://doi.org/10.1055/s-0032-1308999.

Miyano, M., Sayaman, R.W., Stoiber, M.H., Lin, C.H., Stampfer, M.R., Brown, J.B., LaBarge, M.A., 2017. Age-related gene expression in luminal epithelial cells is driven by a microenvironment made from myoepithelial cells. Aging (Albany. NY) 9, 2025–2050. https://doi.org/10.18632/aging.101298.

Monteiro, F.L., Direito, I., Helguero, L.A., 2020. Hormone signaling pathways in the postnatal mammary gland. In: Silva, J.V., Fardilha, M., Freitas, M.J. (Eds.), Tissue-Specific Cell Signal. Springer, pp. 279–315. https://doi.org/10.1007/978-3-030-44436-5.

Mørch, L.S., Skovlund, C.W., Hannaford, P.C., Iversen, L., Fielding, S., Lidegaard, Ø., 2017. Contemporary hormonal contraception and the risk of breast cancer. N. Engl. J. Med. 377, 2228–2239. https://doi.org/10.1056/nejmoa1700732.

Oakes, S.R., Gallego-Ortega, D., Ormandy, C.J., 2014. The mammary cellular hierarchy and breast cancer. Cell. Mol. Life Sci. 71, 4301–4324. https://doi.org/10.1007/s00018-014-1674-4.

Oh, H., Bodelon, C., Palakal, M., Chatterjee, N., Sherman, M.E., Linville, L., Geller, B.M., Vacek, P.M., Weaver, D.L., Chicoine, R.E., Papathomas, D., Patel, D.A., Xiang, J., Clare, S.E., Visscher, D.W., Mies, C., Hewitt, S.M., Brinton, L.A., Storniolo, A.M.V., He, C., Garcia-Closas, M., Chanock, S.J., Gierach, G.L., Figueroa, J.D., 2016. Ages at menarche- and menopause-related genetic variants in relation to terminal duct lobular unit involution in normal breast tissue. Breast Cancer Res. Treat. 158, 341–350. https://doi.org/10.1007/s10549-016-3859-z.

Oral, D., Erkekoglu, P., Kocer-Gumusel, B., Chao, M.W., 2016. Epithelial-mesenchymal transition: a special focus on phthalates and bisphenol A. J. Environ. Pathol. Toxicol. Oncol. 35, 43–58. https://doi.org/10.1615/JEnvironPatholToxicolOncol.2016014200.

Paine, I.S., Lewis, M.T., 2017. The terminal end bud: the little engine that could. J. Mammary Gland Biol. Neoplasia 22, 93–108. https://doi.org/10.1007/s10911-017-9372-0.

Paterni, I., Granchi, C., Minutolo, F., 2017. Risks and benefits related to alimentary exposure to xenoestrogens. Crit. Rev. Food Sci. Nutr. 57, 3384–3404. https://doi.org/10.1080/10408398.2015.1126547.

Pellacani, D., Bilenky, M., Kannan, N., Heravi-Moussavi, A., Knapp, D.J.H.F., Gakkhar, S., Moksa, M., Carles, A., Moore, R., Mungall, A.J., Marra, M.A., Jones, S.J. M., Aparicio, S., Hirst, M., Eaves, C.J., 2016. Analysis of normal human mammary epigenomes reveals cell-specific active enhancer states and associated transcription factor networks. Cell Rep. 17, 2060–2074. https://doi.org/10.1016/j.celrep.2016.10.058.

Pierceall, W.E., Wolfe, M., Suschak, J., Chang, H., Chen, Y., Sprott, K.M., Kutok, J.L., Quan, S., Weaver, D.T., Ward, B.E., 2011. Strategies for H-score normalization of preanalytical technical variables with potential utility to immunohistochemical-based biomarker quantitation in therapeutic reponse diagnostics. Anal. Cell. Pathol. 34, 159–168. https://doi.org/10.1155/2011/583182.

Pu, X., Storr, S.J., Zhang, Y., Rakha, E.A., Green, A.R., Ellis, I.O., Martin, S.G., 2017. Caspase-3 and caspase-8 expression in breast cancer: caspase-3 is associated with survival. Apoptosis 22, 357–368. https://doi.org/10.1007/s10495-016-1323-5.

Puppe, J., Opdam, M., Schouten, P.C., Jozwiak, K., Lips, E., Severson, T., van de Ven, M., Brambillasca, C., Bouwman, P., van Tellingen, O., Bernards, R., Wesseling, J., Eichler, C., Thangarajah, F., Malter, W., Pandey, G.K., Ozretic, L., Caldas, C., van Lohuizen, M., Hauptmann, M., Rhiem, K., Hahnen, E., Reinhardt, H.C., Buttner, R., Mallmann, P., Schomig-Markiefka, B., Schmutzler, R., Linn, S., Jonkers, J., 2019. EZH2 is overexpressed in BRCA1-like breast tumors and predictive for sensitivity to high-dose platinum-based chemotherapy. Clin. Cancer Res. 25, 4351–4362. https://doi.org/10.1158/1078-0432.CCR-18-4024.

Qin, X.Y., Fukuda, T., Yang, L., Zaha, H., Akanuma, H., Zeng, Q., Yoshinaga, J., Sone, H., 2012. Effects of bisphenol A exposure on the proliferation and senescence of normal human mammary epithelial cells. Cancer Biol. Ther. 13, 296–306. https://doi.org/10.4161/cbt.18942.

Raafat, A.M., Hofseth, L.J., Li, S., Bennett, J.M., Haslam, S.Z., 1999. A mouse model to study the effects of hormone replacement therapy on normal mammary gland during menopause: enhanced proliferative response to estrogen in late postmenopausal mice. Endocrinology 140, 2570–2580. https://doi.org/10.1210/endo.140.6.6634.

Raafat, A., Strizzi, L., Lashin, K., Ginsburg, E., McCurdy, D., Salomon, D., Smith, G.H., Medina, D., Callahan, R., 2012. Effects of age and parity on mammary gland lesions and progenitor cells in the FVB/N-RC mice. PLoS One 7, 1–8. https://doi.org/10.1371/journal.pone.0043624.

Reid, B.M., Vyas, S., Chen, Z., Chen, A., Kanetsky, P.A., Permuth, J.B., Sellers, T.A., Saglam, O., 2021. Morphologic and molecular correlates of EZH2 as a predictor of platinum resistance in high-grade ovarian serous carcinoma. BMC Cancer 21, 1–14. https://doi.org/10.1186/s12885-021-08413-3.

Rodgers, K.M., Udesky, J.O., Rudel, R.A., Brody, J.G., 2018. Environmental chemicals and breast cancer: an updated review of epidemiological literature informed by biological mechanisms. Environ. Res. 160, 152–182. https://doi.org/10.1016/j.envres.2017.08.045.

Ruggiero, R.J., Likis, F.E., 2002. Estrogen: physiology, pharmacology, and formulations for replacement therapy. J. Midwifery Wom. Health 47, 130–138. https://doi.org/10.1016/S1526-9523(02)00233-7.

Ruiz, T.F.R., Colleta, S.J., Leonel, E.C.R., Taboga, S.R., 2021a. Mammary carcinoma in aged gerbil mothers after endocrine disruption in pregnancy and lactation. Endocr. Relat. Cancer. https://doi.org/10.1530/ERC-21-0198.

Ruiz, T.F.R., Colleta, S.J., Zuccari, D.A.P.C., Vilamaior, P.S.L., Leonel, E.C.R., Taboga, S.R., 2021b. Hormone receptor expression in aging mammary tissue and carcinoma from a rodent model after xenoestrogen disruption. Life Sci. 285, 120010. https://doi.org/10.1016/j.lfs.2021.120010.

Ruiz, T.F.R., Colleta, S.J., Leonel, E.C.R., Taboga, S.R., 2021c. Mammary carcinoma in aged gerbil mothers after endocrine disruption in pregnancy and lactation. Endocr. Relat. Cancer 28, 715–730. https://doi.org/10.1530/ERC-21-0198.

Ruiz, T.F.R., Leonel, E.C.R., Colleta, S.J., Bedolo, C.M., Pegorin de Campos, S.G., Taboga, S.R., 2022. Gestational and lactational xenoestrogen exposure disrupts morphology and inflammatory aspects in mammary gland of gerbil mothers during involution. Environ. Toxicol. Pharmacol. 89. https://doi.org/10.1016/j.etap.2021.103785.

Ruiz, T.F.R., Vilamaior, P.S.L., Grigio, V., Colleta, S.J., Zucão, M.I., de Campos, S.G.P., dos Santos, F.C.A., Biancardi, M.F., Perez, A.P.S., Taboga, S.R., Leonel, E.C.R., 2023a. The Mongolian gerbil as a useful experimental model in reproductive biology. Reprod. Sci. 30, 2092–2106. https://doi.org/10.1007/s43032-023-01171-6.

Ruiz, T.F.R., Colleta, S.J., dos Santos, D.D., Castro, N.F.C., Cabral, Á.S., Calmon, M.F., Rahal, P., Gil, C.D., Girol, A.P., Vilamaior, P.S.L., Leonel, E.C.R., Taboga, S.R., 2023b. Bisphenol A disruption promotes mammary tumor microenvironment via phenotypic cell polarization and inflammatory response. Cell Biol. Int. 47, 1136–1146. https://doi.org/10.1002/cbin.12007.

Santen, R.J., Allred, D.C., Ardoin, S.P., Archer, D.F., Boyd, N., Braunstein, G.D., Burger, H.G., Colditz, G.A., Davis, S.R., Gambacciani, M., Gower, B.A., Henderson, V. W., Jarjour, W.N., Karas, R.H., Kleerekoper, M., Lobo, R.A., Manson, J.A.E., Marsden, J., Martin, K.A., Martin, L., Pinkerton, J.A.V., Rubinow, D.R., Teede, H., Thiboutot, D.M., Utian, W.H., 2010. Postmenopausal hormone therapy: an endocrine society scientific statement. J. Clin. Endocrinol. Metab. 95, s1–s66. https://doi.org/10.1210/jc.2009-2509.

Schulmeyer, C.E., Fasching, P.A., Häberle, L., Meyer, J., Schneider, M., Wachter, D., Ruebner, M., Pöschke, P., Beckmann, M.W., Hartmann, A., Erber, R., Gass, P., 2023. Expression of the immunohistochemical markers CK5, CD117, and EGFR in molecular subtypes of breast cancer correlated with prognosis. Diagnostics 13. https://doi.org/10.3390/diagnostics13030372.

Segovia-Mendoza, M., Nava-Castro, K.E., Palacios-Arreola, M.I., Garay-Canales, C., Morales-Montor, J., 2020. How microplastic components influence the immune system and impact on children health: focus on cancer. Birth Defects Res 112, 1341–1361. https://doi.org/10.1002/bdr2.1779.

Shafei, A., Ramzy, M.M., Hegazy, A.I., Husseny, A.K., El-hadary, U.G., Taha, M.M., Mosa, A.A., 2018. The molecular mechanisms of action of the endocrine disrupting chemical bisphenol A in the development of cancer. Gene 647, 235–243. https://doi.org/10.1016/j.gene.2018.01.016.

Shalabi, S.F., Miyano, M., Sayaman, R.W., Lopez, J.C., Jokela, T.A., Todhunter, M.E., Hinz, S., Garbe, J.C., Stampfer, M.R., Kessenbrock, K., Seewaldt, V.E., LaBarge, M.A., 2021. Evidence for accelerated aging in mammary epithelia of women carrying germline BRCA1 or BRCA2 mutations. Nat. Aging 1, 838–849. https://doi.org/10.1038/s43587-021-00104-9.

Sikandar, S.S., Kuo, A.H., Kalisky, T., Cai, S., Zabala, M., Hsieh, R.W., Lobo, N.A., Scheeren, F.A., Sim, S., Qian, D., Dirbas, F.M., Somlo, G., Quake, S.R., Clarke, M.F., 2017. Role of epithelial to mesenchymal transition associated genes in mammary gland regeneration and breast tumorigenesis. Nat. Commun. 8, 1–9. https://doi.org/10.1038/s41467-017-01666-2.

Sirka, O.K., Shamir, E.R., Ewald, A.J., 2018. Myoepithelial cells are a dynamic barrier to epithelial dissemination. J. Cell Biol. 217, 3368–3381. https://doi.org/10.1083/JCB.201802144.

Son, H., Moon, A., 2013. Epithelial-mesenchymal transition and cell invasion. Toxicol. Res. 26, 245–252. https://doi.org/10.5487/TR.2010.26.4.245.

Sood, R., Faubion, S.S., Kuhle, C.L., Thielen, J.M., Shuster, L.T., 2014. Prescribing menopausal hormone therapy: an evidence-based approach. Int. J. Womens. Health. 6, 47–57. https://doi.org/10.2147/IJWH.S38342.

Soto, A.M., Brisken, C., Schaeberle, C., Sonnenschein, C., 2013. Does cancer start in the womb? Altered mammary gland development and predisposition to breast cancer due to in utero exposure to endocrine disruptors. J. Mammary Gland Biol. Neoplasia 18, 199–208. https://doi.org/10.1007/s10911-013-9293-5.

Stanko, J.P., Fenton, S.E., 2017. Quantifying branching density in rat mammary gland whole-mounts using the sholl analysis method. J. Vis. Exp. 2017, 1–12. https://doi.org/10.3791/55789.

Stanko, J.P., Easterling, M.R., Fenton, S.E., 2015. Application of sholl analysis to quantify changes in growth and development in rat mammary gland whole mounts. Reprod. Toxicol. 54, 129–135. https://doi.org/10.1016/j.reprotox.2014.11.004.

Sternlicht, M.D., Kouros-Mehr, H., Lu, P., Werb, Z., 2006. Hormonal and local control of mammary branching morphogenesis. Differentiation 74, 365–381. https://doi.org/10.1111/j.1432-0436.2006.00105.x.

Stingl, J., 2011. Estrogen and progesterone in normal mammary gland development and in cancer. Horm. Cancer. 2, 85–90. https://doi.org/10.1007/s12672-010-0055-1.

Stingl, J., Raouf, A., Emerman, J.T., Eaves, C.J., 2005. Epithelial progenitors in the normal human mammary gland. J. Mammary Gland Biol. Neoplasia 10, 49–59. https://doi.org/10.1007/s10911-005-2540-7.

Stuenkel, C.A., 2015. Menopausal hormone therapy: current considerations. Endocrinol. Metab. Clin. North Am. 44, 565–585. https://doi.org/10.1016/j.ecl.2015.05.006.

Stuenkel, C.A., Davis, S.R., Gompel, A., Lumsden, M.A., Murad, M.H., Pinkerton, J.A.V., Santen, R.J., 2015. Treatment of symptoms of the menopause: an endocrine society clinical practice guideline. J. Clin. Endocrinol. Metab. 100, 3975–4011. https://doi.org/10.1210/jc.2015-2236.

Suriyamurthy, S., Baker, D., Ten Dijke, P., Iyengar, P.V., 2019. Epigenetic reprogramming of TGF-β signaling in breast cancer. Cancers (Basel) 11. https://doi.org/10.3390/cancers11050726.

Tarulli, G.A., Laven-Law, G., Shehata, M., Walters, K.A., Denis, I.M., Rahman, M.M., Handelsman, D.J., Dean, N.R., Tilley, W.D., Hickey, T.E., 2019. Androgen receptor signalling promotes a luminal phenotype in mammary epithelial cells. J. Mammary Gland Biol. Neoplasia 24, 99–108. https://doi.org/10.1007/s10911-018-9406-2.

Tawfik, O., Kimler, B.F., Davis, M., Stasik, C., Lai, S.M., Mayo, M.S., Fan, F., Donahue, J. K., Damjanov, I., Thomas, P., Connor, C., Jewell, W.R., Smith, H., Fabian, C.J., 2007. Grading invasive ductal carcinoma of the breast: advantages of using automated proliferation index instead of mitotic count. Virchows Arch. 450, 627–636. https://doi.org/10.1007/s00428-007-0400-0.

Terry, M.B., Michels, K.B., Brody, J.G., Byrne, C., Chen, S., Jerry, D.J., Malecki, K.M.C., Martin, M.B., Miller, R.L., Neuhausen, S.L., Silk, K., Trentham-Dietz, A., McDonald, J., Oskar, S., Knight, J., Toro-Campos, R., Cai, X., Rising, C.J., Afanaseva, D., Mullis, M.D., Berry, M.P., Bird, J., Bradfield, C., Gangnon, R., Gould, M., Hampton, J., Lindberg, S., Luongo, S., Rolland, B., Shull, J., Gaudet, M., Thornquist, M., Aupperlee, M.D., Haslam, S.Z., Hoshyar, R., Kariagina, A., Lopes, J. R., Miller, K.J., Morozova, O., Newkirk, C.J., Schwartz, R.C., Thomas, B., Totzkay, D., Xie, F., Silk, K.J., Biro, F.M., Fassler, C.S., Giannini, C.M., Pinney, S., Troester, M.A., Burke, K., Herbstman, J., Kehm, R., Lilge, L., Perera, F., Sahay, D., Tehranifar, P., Walker, D., Zeinomar, N., De Hoz, M., Shepard, P., Binder, A., Bessonneau, V., De La Rosa, V., Ohayon, J., Rudel, R., Corvalan, C., Pereira, A., Pereira, J., Russo, J., Yanrong, S., Shepherd, J., Adams-Campbell, L., Dash, C., Haddad, B., Hamilton, R., Richardson, B., Denic-Roberts, H., Chang, G., Ding, Y.C., Kanaya, N., Rakoff, M., Saeki, K., Serrano, M., Reynolds, P., Dunphy, K., Jerry, J., Symington, A., Vandenberg, L., Schneider, S., Adams, S.A., Brandt, H.M., Friedman, D., Lead, J.R., Kreps, G., Wright, K., Burke-Garcia, A., Fisher, C., 2019. Environmental exposures during windows of susceptibility for breast cancer: a framework for prevention research. Breast Cancer Res. 21, 1–16. https://doi.org/10.1186/s13058-019-1168-2.

Thompson, M.E., 2010. BRCA1 16 years later: nuclear import and export processes. FEBS J. 277, 3072–3078. https://doi.org/10.1111/j.1742-4658.2010.07733.x.

Tolg, C., Cowman, M., Turley, E., 2018. Mouse mammary gland whole mount preparation and analysis. Bio-Protocol 8, 1–8. https://doi.org/10.21769/bioprotoc.2915.

Tsuda, H., Tani, Y., Weisenberger, J., Kitada, S., Hasegawa, T., Murata, T., Tamai, S., Hirohashi, S., Matsubara, O., Natori, T., 2005a. Frequent KIT and epidermal growth factor receptor overexpressions in undifferentiated-type breast carcinomas with 'stem-cell-like' features. Cancer Sci. 96, 333–339. https://doi.org/10.1111/j.1349-7006.2005.00060.x.

Tsuda, H., Morita, D., Kimura, M., Shinto, E., Ohtsuka, Y., Matsubara, O., Inazawa, J., Tamaki, K., Mochizuki, H., Tamai, S., Hiraide, H., 2005b. Correlation of KIT and EGFR overexpression with invasive ductal breast carcinoma of the solid-tubular subtype, nuclear grade 3, and mesenchymal or myoepithelial differentiation. Cancer Sci. 96, 48–53. https://doi.org/10.1111/j.1349-7006.2005.00009.x.

V Fernandez, S., Huang, Y., Snider, K.E., Zhou, Y., Pogash, T.J., Russo, J., 2012. Expression and DNA methylation changes in human breast epithelial cells after bisphenol A (BPA) exposure. Int. J. Oncol. 41, 369–377. https://doi.org/10.3892/ijo.2012.1444.

Vabre, P., Gatimel, N., Moreau, J., Gayrard, V., Picard-Hagen, N., Parinaud, J., Leandri, R.D., 2017. Environmental pollutants, a possible etiology for premature ovarian insufficiency: a narrative review of animal and human data. Environ. Heal. A Glob. Access Sci. Source. 16, 1–18. https://doi.org/10.1186/s12940-017-0242-4.

Visvader, J.E., Stingl, J., 2014. Mammary stem cells and the differentiation hierarchy: current status and perspectives. Genes Dev. 28, 1143–1158. https://doi.org/10.1101/gad.242511.114.

Vougiouklakis, T., Belovarac, B.J., Lytle, A., Chiriboga, L., Ozerdem, U., 2020. The diagnostic utility of EZH2 H-score and Ki-67 index in non-invasive breast apocrine lesions. Pathol. Res. Pract. 216, 153041. https://doi.org/10.1016/j.prp.2020.153041.

Wang, L., Di, L.J., 2014. BRCA1 and estrogen/estrogen receptor in breast cancer: where they interact? Int. J. Biol. Sci. 10, 563–573. https://doi.org/10.7150/ijbs.8579.

Wang, K.H., Kao, A.P., Chang, C.C., Lin, T.C., Kuo, T.C., 2013. Bisphenol A at environmentally relevant doses induces cyclooxygenase-2 expression and promotes invasion of human mesenchymal stem cells derived from uterine myoma tissue. Reprod. Toxicol. 52, 229–233. https://doi.org/10.1016/j.tjog.2013.04.016.

Wang, C., Qu, L., Li, S., Yin, F., Ji, L., Peng, W., Luo, H., Lu, D., Liu, X., Chen, X., Kong, L., Wang, X., 2021. Discovery of first-in-class dual PARP and EZH2 inhibitors for triple-

negative breast cancer with wild-type BRCA. J. Med. Chem. 64, 12630–12650. https://doi.org/10.1021/acs.jmedchem.1c00567.

Zhao, N., Powell, R.T., Yuan, X., Bae, G., Roarty, K.P., Stossi, F., Strempfl, M., Toneff, M. J., Johnson, H.L., Mani, S.A., Jones, P., Stephan, C.C., Rosen, J.M., 2021. Morphological screening of mesenchymal mammary tumor organoids to identify drugs that reverse epithelial-mesenchymal transition. Nat. Commun. 12, 1–13. https://doi.org/10.1038/s41467-021-24545-3.

Zheng, L., Zhou, B., Meng, X., Zhu, W., Zuo, A., Wang, X., Jiang, R., Yu, S., 2014. A model of spontaneous mouse mammary tumor for human estrogen receptor- and progesterone receptor-negative breast cancer. Int. J. Oncol. 45, 2241–2249. https://doi.org/10.3892/ijo.2014.2657.